© 2015. Published by The Company of Biologists Ltd | Development (2015) 142, 140-150 doi:10.1242/dev.104927

RESEARCH ARTICLE

Thalamic afferents influence cortical progenitors via ephrin A5-EphA4 interactions

Katrin Gerstmann[1,2,*], Daniel Pensold[1,*], Judit Symmank[1], Mukhran Khundadze[1], Christian A. Hübner[1], Jürgen Bolz[2] and Geraldine Zimmer[1,2,‡]

ABSTRACT

The phenotype of excitatory cerebral cortex neurons is specified at the progenitor level, orchestrated by various intrinsic and extrinsic factors. Here, we provide evidence for a subcortical contribution to cortical progenitor regulation by thalamic axons via ephrin A5-EphA4 interactions. Ephrin A5 is expressed by thalamic axons and represents a high-affinity ligand for EphA4 receptors detected in cortical precursors. Recombinant ephrin A5-Fc protein, as well as ephrin A ligand-expressing, thalamic axons affect the output of cortical progenitor division *in vitro*. Ephrin A5-deficient mice show an altered division mode of radial glial cells (RGCs) accompanied by increased numbers of intermediate progenitor cells (IPCs) and an elevated neuronal production for the deep cortical layers at E13.5. In turn, at E16.5 the pool of IPCs is diminished, accompanied by reduced rates of generated neurons destined for the upper cortical layers. This correlates with extended infragranular layers at the expense of superficial cortical layers in adult ephrin A5-deficient and EphA4-deficient mice. We suggest that ephrin A5 ligands imported by invading thalamic axons interact with EphA4-expressing RGCs, thereby contributing to the fine-tuning of IPC generation and thus the proper neuronal output for cortical layers.

KEY WORDS: Ephrin A5, Neurogenesis, Cortex, Thalamus

INTRODUCTION

The excitatory projection neurons of the different cortical layers are generated in a temporal fashion, with deep layer neurons born first, while upper layer neurons are produced later during corticogenesis, regulated by a complex network of intrinsic and extrinsic mechanisms (Franco and Muller, 2013).

Two main types of cortical progenitors are described. Radial glial cells (RGCs) characterized by Pax6 expression and a defined apicobasal polarity reside in the ventricular zone (VZ) and undergo asymmetric divisions at the onset of neurogenesis, generating neurons directly or predominantly indirectly by producing a second type of precursor termed the intermediate progenitor cells (IPCs) (Chenn and McConnell, 1995; Rao et al., 2000; Kriegstein and Gotz, 2003; Gotz and Huttner, 2005). Tbr2-positive IPCs translocate to the subventricular zone (SVZ) and undergo symmetric divisions, producing either pairs of neurons or self-amplifying prior to neurogenesis, contributing to all cortical layers (Haubensak et al., 2004; Noctor et al., 2004, 2008; Englund et al., 2005; Attardo et al., 2008; Farkas et al., 2008; Sessa et al., 2008; Kowalczyk et al., 2009; Vasistha et al., 2014).

Endogenous regulation of cortical neurogenesis by transcription factors and morphogens, feedback signaling by postmitotic neurons and the regulation of neuronal progenitors by meninges as well as factors of the liquor have all been described (Siegenthaler and Miller, 2008; Seuntjens et al., 2009; Lehtinen and Walsh, 2011; Tiberi et al., 2012; Parthasarathy et al., 2014; Toma et al., 2014). Moreover, paracrine interactions of membrane-bound molecules, such as the Eph/ephrin system, affect the proliferation and differentiation of cortical progenitors (Qiu et al., 2008; North et al., 2009).

Eph-ephrin interactions regulate a variety of neurodevelopmental processes, including axonal guidance, migration and apoptosis, in addition to proliferation (Drescher et al., 1997; Flanagan and Vanderhaeghen, 1998; Depaepe et al., 2005; Zimmer et al., 2008; North et al., 2009; Rudolph et al., 2010), and are crucial for establishing thalamocortical projections (Donoghue and Rakic, 1999; Šestan et al., 2001; Bolz et al., 2004).

Despite intensive discussion as to whether cortical development is mainly regulated by intrinsic and/or extrinsic cues (Rakic, 1988, 1991; Dehay et al., 2001; Rakic et al., 2009; Zhou et al., 2010; Reillo et al., 2011), the thalamic influence on cortical progenitors and neurogenesis remains debated. Here, we provide further evidence for the extra-cortical regulation of cortical progenitors and hence the final output of neurons by thalamic afferents via the Eph/ephrin system.

RESULTS

The cortical architecture is affected in ephrin A5-deficient and EphA4-deficient mice

Ephrin A5 is expressed in cortical tissue at embryonic as well as postnatal stages (Fig. 1A; supplementary material Fig. S1A). Here, we aimed to address the role of ephrin A5 during cortical neurogenesis and in neocortical organization in adult mice.

We first analyzed radial extension of the cortical layers of the somatosensory cortex of adult ephrin A5-deficient and wild-type mice at postnatal day (P) 37. We performed DAPI staining of coronal brain sections in combination with immunolabeling, using antibodies directed against Cux2 (Nieto et al., 2004; Zimmer et al., 2004) and Otx1/2 (Frantz and McConnell, 1996) to distinguish between the superficial and infragranular layers, respectively. This analysis revealed a significant increase in the radial extension of deep layers V and VI in ephrin A5 knockout animals, compared with wild types, at the expense of radial extension of superficial layers II-IV at P37 (Fig. 1C-E). The overall cortical thickness remained unchanged (supplementary material Fig. S1B). The neuronal density of the different layers, as determined by the number of NeuN (Rbfox3)-labeled neurons among DAPI-stained cells, revealed no significant

[1]Institute of Human Genetics, Jena University Hospital, Friedrich-Schiller-University Jena, 07743 Jena, Germany. [2]Institute for General Zoology and Animal Physiology, Friedrich-Schiller-University Jena, 07743 Jena, Germany.
*These authors contributed equally to this work

‡Author for correspondence (geraldine.zimmer@med.uni-jena.de)

Received 15 October 2013; Accepted 27 October 2014

Development (2015) 142, 140-150 doi:10.1242/dev.104927

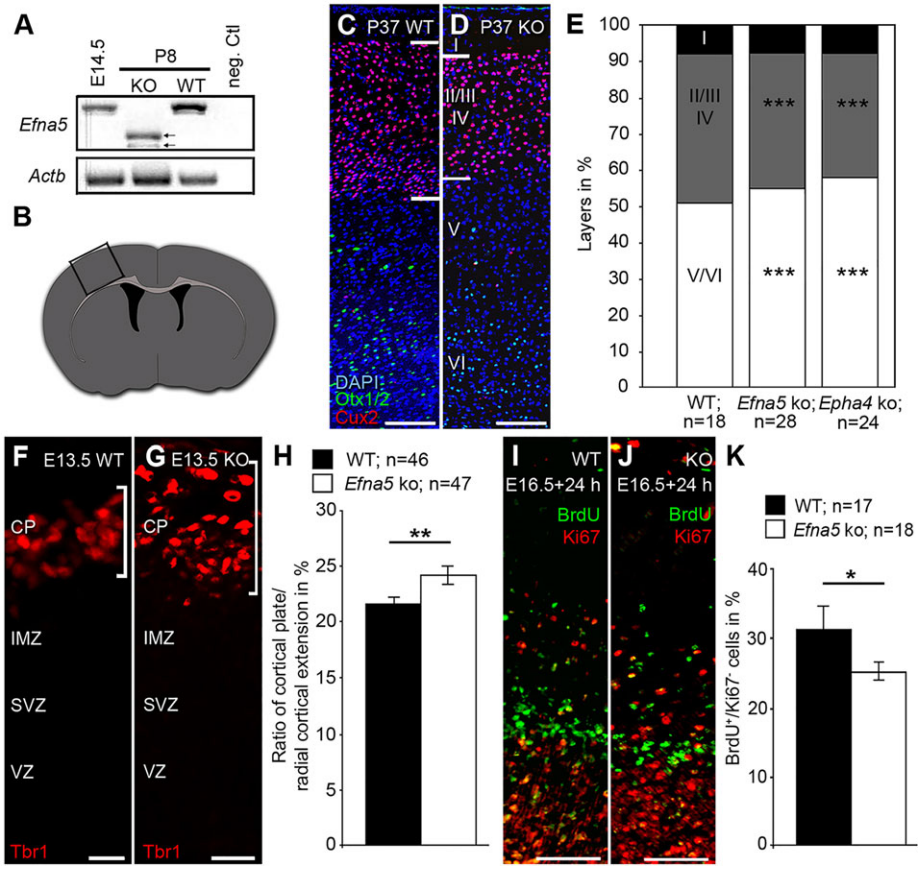

Fig. 1. Ephrin A5 contributes to the regulation of cortical neurogenesis. (A) RT-PCR of cortical tissue from E14.5 wild-type (WT) and from P8 WT and ephrin A5 knockout (KO) brains with β-actin (*Actb*) and ephrin A5 (*Efna5*) primers shows ephrin A5-expression in the developing and adult wild-type cortex. neg. Ctl., negative control that lacks DNA. The arrows point to different truncated splicing variants in knockout mice. (B) Schematic illustration of the anterior-posterior level of the adult coronal brain sections used for analysis (bregma: zero). The box indicates the cortical region analyzed. (C-E) Triple labeling with DAPI (blue) and for Cux2 (red) and Otx1/2 (green) in coronal sections of P37 wild-type (C) and ephrin A5 knockout (D) cortex to determine radial extensions of the cortical layers I, II-IV and V/VI. (E) Quantitative analysis of the relative thickness of the P37 cortical layers revealed increased infragranular layers V/VI and reduced superficial layers II-IV in ephrin A5-deficient mice (five brains) compared with wild types (four brains). Similar results were obtained for the comparison of layer I (n.s., $P>0.05$), layers II-IV and layers V/VI between wild-type (four brains) and *Epha4* knockout (three brains) mice. ***$P<0.001$, one-way ANOVA and Bonferroni's multiple comparisons test. (F-H) Tbr1 immunostaining of E13.5 coronal sections of wild-type (F) and ephrin A5 mutant (G) brains. (H) Quantitative analysis of the radial extension of Tbr1-positive cells, representing the cortical plate, in relation to radial extension of the cortex. **$P<0.01$, Student's *t*-test; three brains per genotype. (I-K) The number of neurons exiting the cell cycle decreased significantly in ephrin A5 knockout (J) compared with wild-type (I) brains as shown by BrdU/Ki67 labeling 24 h after BrdU application at E16.5. (K) Quantitative analysis of cell cycle exit. *$P\leq0.05$, Student's *t*-test; three brains per genotype. In E,H,K, *n* refers to the number of sections analyzed. Error bars (H,K) indicate s.e.m. VZ, ventricular zone; SVZ, subventricular zone; IMZ, intermediate zone; CP, cortical plate. Scale bars: 100 µm in C,D; 50 µm in F,G,I,J.

alterations in the ephrin A5-deficient cortices (supplementary material Fig. S1C-E).

To determine if the phenotype is caused by an accumulation of neurons fated for the supragranular layers in deep layers, BrdU birthdating experiments were performed. BrdU administration at E16.5, when supragranular layer neurons are born, did not reveal ectopically located BrdU-positive neurons in the deep layers of the adult cortex (supplementary material Fig. S1F-H). However, consistent with the increased thickness of the deep layers at the expense of the upper layers, the E16.5 BrdU-labeled cells were shifted towards the pial surface in adults (supplementary material Fig. S1F-H).

Interestingly, the radial extension of the deep layers at the expense of the upper cortical layers observed in ephrin A5 mutants was phenocopied by *Epha4* knockout mice (Fig. 1E). This suggests that EphA4 is the mediating receptor and that ephrin A5-EphA4 interactions contribute to the regulation of developmental processes underlying proper cortical layering.

Neuronal output is increased early and reduced at later stages of neurogenesis in ephrin A5 mutant mice

How does ephrin A5 deficiency affect cortical development resulting in altered cortical layer thickness? The Eph/ephrin system regulates apoptosis of early cortical progenitors at E11 and E12 (Depaepe et al., 2005). However, we did not observe any alterations in the number of caspase 3-positive cells in the embryonic cortex at E13.5 and E16.5 of ephrin A5-deficient mice (supplementary material Fig. S2B-C′). When a TUNEL-based apoptosis assay was performed with E14.5 cortical cells plated on a substrate of recombinant ephrin A5-Fc, or of Fc as control, no difference in the number of apoptotic cells was determined after 5 h *in vitro* (13.6±3.3%, $n=245$ for ephrin A5-Fc and 15.9±4.4%, $n=145$ for control; n.s., $P=0.52$).

Next, we assessed whether the altered radial layer extensions in adult ephrin A5-deficient mice are elicited by changes in cortical neurogenesis. We focused our analysis predominantly on E13.5 and E16.5, when deep versus upper layer neurons are born (Polleux

Development (2015) 142, 140-150 doi:10.1242/dev.104927

et al., 1997), and examined the dorsolateral cortex of coronal brain sections of the same anterior posterior level, characterized by the appearance of the medial and lateral ganglionic eminence in the basal telencephalon (supplementary material Fig. S2A). To monitor whether the expansion of deep layers results from an increase in neuronal production at E13.5, we performed immunostaining against Tbr1 as a marker for early postmitotic neurons (Englund et al., 2005; Kolk et al., 2005). The radial extension of Tbr1-positive cells in the dorsolateral cortex representing the cortical plate (CP) at E13.5 was measured in relation to overall cortical thickness. Indeed, compared with wild type, a significant increase in Tbr1-positive cells was observed in ephrin A5-deficient brain sections (Fig. 1F-H). This correlates with augmented numbers of Tbr1-positive cells per unit area, increasing from 24.4±1.1 cells in wild-type (n=46) to 28.9±1.2 in ephrin A5-deficient (n=47) embryos ($P \leq 0.01$, three brains per genotype). These results suggest that the number of postmitotic neurons was increased in E13.5 ephrin A5-deficient cortices.

In agreement with the augmented numbers of postmitotic neurons at E13.5, we also revealed an increase in overall cortical thickness in E13.5 ephrin A5 mutant embryos (supplementary material Fig. S2D). However, the cortical thickness returned to wild-type levels with progressing embryonic age (supplementary material Fig. S2E-G). This suggests that the elevated generation of neurons is temporally restricted to the stage of early corticogenesis, when deep layer neurons are born.

To quantify the number of postmitotic cells during the generation of superficial layer neurons, we assessed the rate of cells leaving the cell cycle by BrdU pulsing at E16.5 and subsequent BrdU/Ki67 double labeling after 24 h. The BrdU single-labeled cells represent the fraction that left the cell cycle, which was reduced in ephrin A5-deficient mice (Fig. 1I-K). In wild-type embryos we determined 32.94±2.0% BrdU single-labeled cells, whereas a decrease to 26.1±1.7% was determined in ephrin A5-deficient animals (Fig. 1K). This observation points to reduced neuronal production during the generation of upper layer neurons.

We also performed *in situ* hybridization experiments with an insulinoma-associated 1 (*Insm1*)-specific riboprobe at E16.5, to label terminally dividing cells (Farkas et al., 2008; Rosenbaum et al., 2011). *Insm1* expression was detected in cortical proliferative zones of wild-type and ephrin A5 knockout cortices (supplementary material Fig. S2H,I). Decreased signal intensities were revealed in ephrin A5 knockout brains predominantly in the SVZ (supplementary material Fig. S2J). These data indicate that the reduced cell cycle exit observed at later stages (E16.5+24 h) results from diminished neurogenic divisions of IPCs residing in the SVZ.

Ephrin A5 deficiency differentially affects the number of IPCs at distinct embryonic stages

As described above, the altered neuronal output at E13.5 and E16.5 correlates with changes in the thickness of the deep and upper cortical layers in ephrin A5-deficient mice. To analyze whether RGC division is affected in ephrin A5-deficient mice we performed immunostaining against Aspm to label spindle poles in combination with DAPI nuclear staining and analyzed the orientation of the cleavage plane of RGCs in relation to the ventricular surface in ephrin A5-deficient and wild-type embryos (Fig. 2A-A″) (Fish et al., 2006; Asami et al., 2011). In accordance with Asami et al. (2011), the angles of cell division were classified into three groups: with a cleavage plane of 0-30° (horizontal), 30-60° (oblique) or 60-90° (vertical) (Fig. 2B,B′). In wild-type animals, most of the division events analyzed were defined as vertical (59.3%), with 34.5% classified as oblique and 6.2% as horizontal (Fig. 2C). In E13.5 ephrin A5-deficient embryos we detected an 18.2% decrease in vertical divisions to 41.1%, whereas the percentage of obliquely and horizontally dividing apical progenitors increased to 43.3% and 15.6%, respectively (Fig. 2C). These data suggest that ephrin A5 deficiency affects the mode of RGC division, leading to an increase in divisions with unequal inheritance (asymmetric division).

Next, we performed the pair-cell assay as a gain-of-function approach to directly show the effect of exogenously applied ephrin A5-Fc on RGC division. E13.5 cortical cells were plated at clonal density and stimulated with recombinant clustered ephrin A5-Fc or with Fc as control. After 24 h *in vitro*, division of progenitor cells leads to the formation of cell pairs. By staining with antibodies directed against nestin and βIII-tubulin we distinguished between RGCs and postmitotic neurons, respectively. The analysis of cell pairs consisting of either two nestin-positive cells, two βIII-tubulin-positive cells, or one βIII-tubulin-positive and one nestin-positive cell (Fig. 2D-F) revealed a significant increase in the proportion of the mixed βIII-tubulin/nestin-positive combination at the expense of βIII-tubulin-positive postmitotic pairs upon ephrin A5-Fc stimulation (Fig. 2G). The reduction of postmitotic neurons in response to ephrin A5-Fc application is the converse of, and hence consistent with, what we observed in ephrin A5-deficient mice. The pair-cell assay only monitors symmetric proliferative and neurogenic, as well as asymmetric neurogenic, division events. Ephrin A5-dependent changes in asymmetric proliferative divisions leading to the generation of RGC and IPC daughters were not addressed in the pair-cell assay.

Thus, we next examined the appearance of distinct types of cortical progenitors at different embryonic stages in ephrin A5-deficient and wild-type embryos. To distinguish between RGCs and IPCs, we performed immunostainings with antibodies against Pax6 and Tbr2 (Eomes), respectively (Gotz et al., 1998; Englund et al., 2005; Pontious et al., 2008). For quantitative analysis of Pax6-labeled and Tbr2-labeled cells, we divided E13.5 cortices into ten equal horizontal segments, while twenty segments were used for analysis at E16.5 and E18.5, and the cell number per segment was determined. At E13.5, the number of Pax6-expressing RGCs was similar between knockout and wild-type cortices, except for a slight increase restricted to segments 8 and 9 in ephrin A5-deficient mice (supplementary material Fig. S3A-C). As segments 8 and 9 represent regions with high IPC numbers and therefore mainly refer to the SVZ (Fig. 2H-J), the augmentation of RGCs is likely to reflect newly generated IPCs that still express some Pax6 (Englund et al., 2005). Staining for Tbr2-positive IPCs revealed a highly significant increase in segments 3-8 of E13.5 ephrin A5-deficient cortices (Fig. 2H-J), whereby segments 1-7 represent the VZ as illustrated by Pax6 labeling at E13.5 (supplementary material Fig. S3A,B). Hence, the increase in Tbr2-positive cells seems to be caused by a boosted production of IPCs by RGCs, which is consistent with the elevated levels of asymmetric RGC division observed in E13.5 ephrin A5-deficient mice. By contrast, at E16.5 the number of Tbr2-positive progenitors was significantly decreased in segments 6 and 8 (Fig. 2K-M), and this became even more evident at E18.5 (Fig. 2N-P), whereas we observed a slight increase in Pax6-positive RGCs in segments 5-7 of the E16.5 ephrin A5-deficient mice (supplementary material Fig. S3D-F).

The changes in the number of RGCs and IPCs at later stages were also reflected in an analysis of the proportional distribution of Ki67-labeled mitotic cells (E16.5) in the VZ and SVZ, where apical versus basal progenitors reside. In ephrin A5-deficient animals, we observed an increase in the proportion of proliferating cells located

Development (2015) 142, 140-150 doi:10.1242/dev.104927

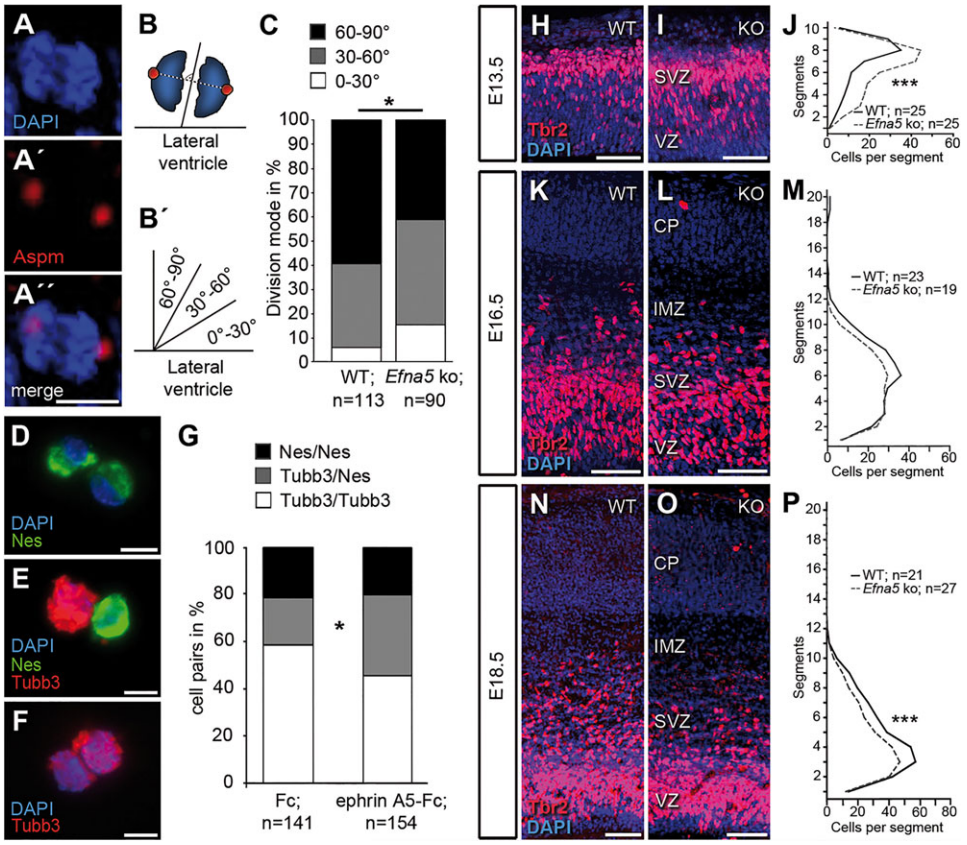

Fig. 2. *Efna5*-deficient mice exhibit alterations in the division mode of RGCs and in IPC numbers. (A-C) The cleavage plane in relation to the ventricular surface of RGCs was determined with Aspm and DAPI staining (A-A″), defining 0-30° as horizontal, 30-60° as oblique and 60-90° as vertical division (B,B′). (C) Decreased vertical and increased horizontal divisions were detected in ephrin A5-deficient mice (*P=0.014, Chi-square test; three brains per genotype). (D-G) Pair-cell assay with E13.5 cortical cells after 24 h *in vitro*. Upon ephrin A5-Fc stimulation the proportion of βIII-tubulin/nestin-positive cell pairs increased (*P<0.05, Student's t-test) at the expense of βIII-tubulin/βIII-tubulin-positive cell pairs, as compared with Fc application (five independent experiments). (H-P) Tbr2 immunostaining in coronal sections of E13.5 embryos revealed augmented numbers of IPCs in the dorsolateral cortex of ephrin A5 knockouts (I) compared with wild types (H) as quantified in J (***P≤0.001, two-way ANOVA). Bonferroni test revealed significantly increased IPC numbers in segments 3-8 (***P≤0.001 for each segment; three brains for wild type and four brains for ephrin A5-deficient embryos). (K-M) At E16.5 a significant reduction of Tbr2-positive cells was observed in the ephrin A5 knockout (L) compared with wild-type (K) coronal sections for segments 6 and 8 as quantified in M (*P≤0.05, Bonferroni test; three brains per genotype). (N-P) The reduction of IPCs in coronal sections of ephrin A5 knockout embryos was even stronger at E18.5 (***P≤0.001, two-way ANOVA; three brains per genotype), showing decreased levels for segments 3-8 with Bonferroni test (***P≤0.001 for segments 3-6; **P≤0.01 for segments 7 and 8); in J and P, the significance of the two-way ANOVA is depicted. n refers to the number of cells (C), cell pairs (G) or sections (J,M,P) analyzed. VZ, ventricular zone; SVZ, subventricular zone; IMZ, intermediate zone; CP, cortical plate; Tubb3, βIII-tubulin; Nes, nestin. Scale bars: 100 µm in N,O; 50 µm in H,I,K,L; 25 µm in D-F; 5 µm in A″.

in the VZ, while Ki67-labeled cells in the SVZ decreased accordingly (supplementary material Fig. S3G-I).

Taken together, ephrin A5-deficient embryos show increased rates of horizontally dividing RGCs accompanied by slightly elevated numbers of Pax6-positive cells at E13.5 and E16.5. Moreover, we detected changes in the IPC pool, with strongly augmented levels at E13.5 and decreased numbers at E16.5 and E18.5, which correlate with the alterations in neuronal production observed in ephrin A5-deficient mice. This suggests that the defects in the adult cortical layers are mainly provoked by the altered pool of IPCs in ephrin A5 knockout mice, which, at least at E13.5, appears to be a consequence of changes in the RGC division mode.

Ephrin A5 ligands induce EphA4 receptor forward signaling in cortical progenitors

As described above, adult *Epha4* knockout mice mimic the alterations in radial layer extension observed in ephrin A5 mutants (Fig. 1E), suggesting that ephrin A5-induced EphA4 forward signaling in cortical progenitors is involved in the regulation of proliferation and differentiation. Indeed, *in situ* hybridization experiments revealed that, of all ephrin A5-interacting receptors, only EphA4 is strongly expressed in the cortical proliferative regions (supplementary material Fig. S4). EphA4 expression could be detected from E13.5-E16.5 (Fig. 3A-C). Immunohistochemistry in coronal brain sections revealed EphA4 localization in the membrane of the soma and along the radial processes of nestin-expressing RGCs spanning the whole radial extension of the developing cortex (Fig. 3D-G‴). Consistent with this, binding studies with Alexa 488-labeled ephrin A5-Fc showed binding sites in the intermediate zone (IMZ) and CP in addition to the proliferative zones in living cortical slice cultures (Fig. 3H). EphA4 expression in nestin-positive RGCs was further directly demonstrated by immunostaining of dissociated cortical cells (Fig. 3I-L).

EphA4 is a high-affinity binding partner for ephrin A5 (Davis et al., 1994). By applying recombinant ephrin A5-Fc clustered with Alexa 488-labeled anti-human IgG to dissociated E14.5 cortical single cells, we showed that ephrin A5-Fc interacts with EphA4 receptors of cortical precursors as identified by Ki67 and EphA4

Development (2015) 142, 140-150 doi:10.1242/dev.104927

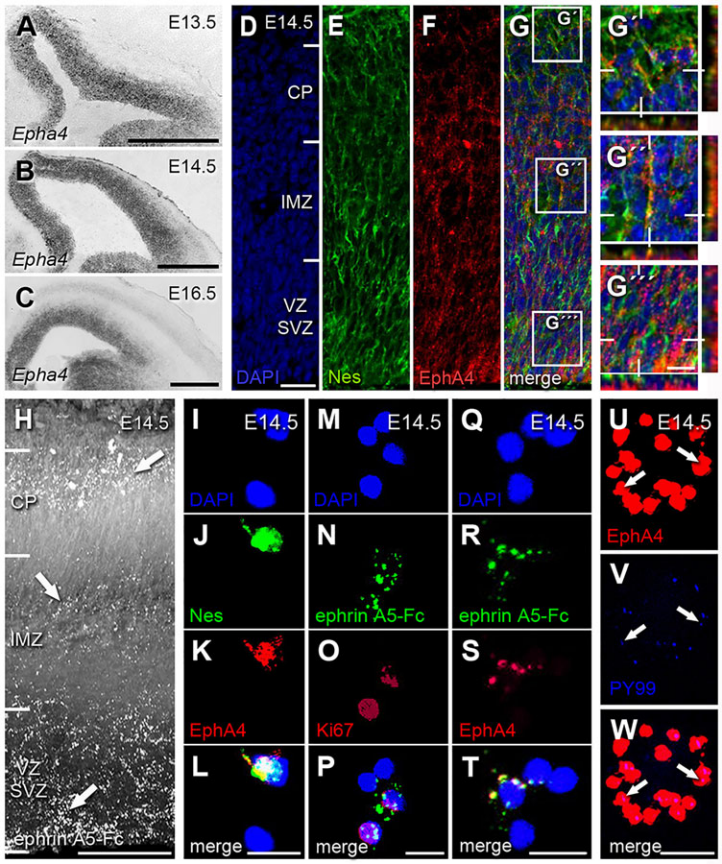

Fig. 3. *EphA4* receptors are expressed by cortical progenitors and can be activated by ephrin A5-Fc. (A-C) *In situ* hybridization against *Epha4* of wild-type coronal brain sections at E13.5 (A), E14.5 (B) and E16.5 (C) labels the proliferative cortical zones. (D-G‴) DAPI staining (D) and nestin (E) and EphA4 (F) immunostaining revealed EphA4 receptors localized in the membrane of the soma and basal processes of cortical progenitors at E14.5 (point-specific colocalization is shown in the ortho *z*-stack in G-G‴). (H) Alexa 488-labeled (white) ephrin A5-Fc binding sites in the cortex of coronal organotypic slice cultures (E14.5+3 h). Arrows point to binding sites in the VZ, IMZ and CP. (I-L) EphA4 immunolabeling was detected in dissociated nestin-positive cells (E14.5+1div). (M-P) Alexa 488-clustered ephrin A5-Fc binds to Ki67-positive cortical precursors (E14.5+1div). (Q-T) Alexa 488-clustered ephrin A5-Fc binding sites colocalized with the immunohistochemical labeling of EphA4 (E14.5+ 1div). (U-W) Activation of EphA4 receptors induced by ephrin A5-Fc stimulation is shown by phosphotyrosine 99 (PY99) immunostaining (E14.5+1div). Arrows indicate colocalisation of PY99 and EphA4 receptor signal. Scale bars: 500 µm in A-C; 100 µm in H; 25 µm in D; 10 µm in G‴,L,P,T; 5 µm in W.

staining (Fig. 3M-T). As illustrated by anti-phosphotyrosine (PY99) labeling, EphA4 receptors of cortical cells were activated upon ephrin A5-Fc stimulation (Fig. 3U-W), which we already reported in a previous study (Zimmer et al., 2007). In summary, these data show EphA4 receptor expression by cortical progenitors, and that these are activated upon ephrin A5-Fc binding.

Ephrin A5 expression is neither detected in cortical progenitors nor in postmitotic neurons

The results presented so far suggest that ephrin A5-induced EphA4 forward signaling in RGCs is involved in the regulation of the pool of IPCs and thus the neuronal output fated for the infra- and supragranular layers. Robust EphA4 expression was observed in cortical progenitors at the mRNA and protein levels. As Eph-ephrin signaling is dependent on cell-cell contact owing to the localization of the proteins in the cell membrane, we next examined which cells express ephrin A5 ligands. Paracrine Eph-ephrin signaling by cortical progenitors has already been described (Qiu et al., 2008; North et al., 2009). Furthermore, a feedback signaling by postmitotic neurons (Seuntjens et al., 2009; Parthasarathy et al., 2014; Toma et al., 2014) also represents a potential mechanism, as EphA4-expressing radial processes of RGCs could serve as a structural scaffold.

Ephrin A5 mRNA was already shown in E14.5 preparations of cortical tissue by RT-PCR (Fig. 1A). Although we observed ephrin A5 expression by non-radioactive *in situ* hybridization in other regions of the developing brain, including the thalamus, it was not detected in cortical structures at E13.5-E16.5 (Fig. 4A-C). To circumvent sensitivity limitations of non-radioactive *in situ* hybridization, we performed single-cell RT-PCR, which provides high sensitivity and cellular resolution. Individual embryonic cortical cells were manually isolated and limited 3′-end cDNA libraries of the transcriptome were generated. With sequence-specific primers against *Pax6*, *Tbr2* and *HuD* (*Elavl4*), we discriminated between RGCs, IPCs and postmitotic neurons, respectively. Whereas EphA4 expression was detected in most of the Pax6-positive RGCs (n=13 of 15 tested cells) as well as in some Tbr2-expressing IPCs (n=4 of 7 tested cells) confirming the data presented above, ephrin A5 was not detected in cortical progenitors (Fig. 4D,E). Furthermore, ephrin A5 transcripts were also absent from single-cell cDNA libraries, which were classified as postmitotic cortical transcriptomes according to HuD expression (Fig. 4F) (Fujiwara et al., 2008; Gauthier-Fisher et al., 2009). However, ephrin A5 was detected in single-cell libraries isolated from the preoptic area known to express this ligand (Fig. 4D,E; n=3) (Zimmer et al., 2008), as well as in cDNAs generated from single-cell-equivalent dilutions (10 pg quantities) of embryonic brain tissue RNA that served as positive controls. Thus, consistent with the results of the *in situ* hybridization experiments shown in Fig. 4A-C, ephrin A5 was not detected in cortical progenitors and postmitotic neurons. Hence, a paracrine EphA4 activation induced by ephrin A5-expressing neighboring cortical precursors or a feedback signaling of postmitotic neurons seems unlikely.

Ephrin A5 is expressed in thalamic axons

Thalamic ephrin A5 mRNA expression at E13.5 was observed in the mantle zone (Fig. 4A, arrow), from which the first axons grow to the developing cortex and which is positive for L1 (L1cam) (Fig. 5I, arrow). Placing a DiI crystal into the E16.5 dorsolateral cortex tags the thalamic ventrobasal complex, a region that corresponds to the ephrin A5-expressing thalamic nuclei at E16.5 and that is known to

Development (2015) 142, 140-150 doi:10.1242/dev.104927

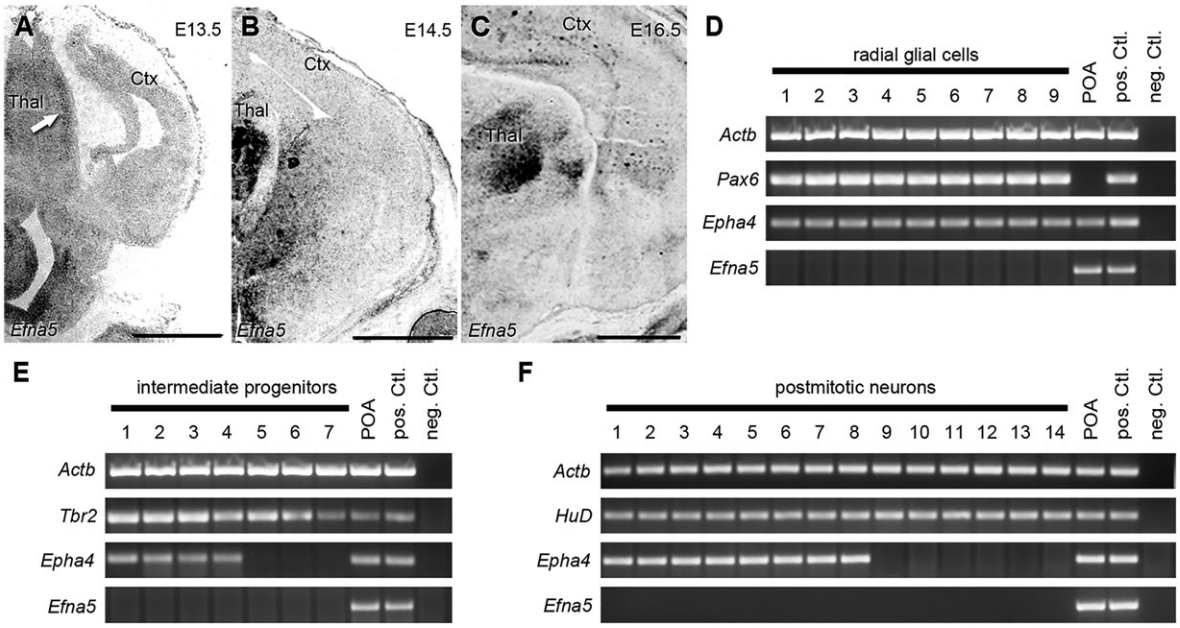

Fig. 4. *Efna5* is not expressed by cortical cells but in the developing thalamus. (A-C) Ephrin A5 mRNA was not detected in the cortex of embryonic coronal brain sections at E13.5 (A), E14.5 (B) and E16.5 (C) by *in situ* hybridization. The developing thalamus shows ephrin A5 expression from E13.5 onwards (A). The arrow in A points to the mantle zone of the thalamus. (D-F) Single-cell RT-PCR of E16.5 cortical progenitors (D,E) and postmitotic cortical neurons (F). Ephrin A5 (*Efna5*) transcripts were absent from cortical progenitors, as identified by *Pax6* expression for RGCs (n=15; D) and by *Tbr2* signal for IPCs (n=7; E), and from *HuD*-expressing postmitotic neurons (n=17; F). Preotic area-derived single-cell libraries (E14.5, n=3; D-F) and cDNA libraries of whole brain tissue RNA (E14.5/E16.5) served as positive controls (pos. Ctl.); the negative control (neg. Ctl.) lacked cDNA. *Epha4* expression in *Pax6*-positive and *Tbr2*-positive cortical progenitors was confirmed at the single-cell level (D,E) and was found in some postmitotic neurons (F). *Actb*, β-actin; Ctx, cortex; POA, preotic area; Thal, thalamus. Scale bars: 500 µm in A-C.

innervate the somatosensory cortex (supplementary material Fig. S5A,B) (Uziel et al., 2006).

At later stages of cortical development ephrin A5 affects the topography and branching of thalamocortical afferents (Bolz et al., 2004). Thus, the effects observed in the ephrin A5 mutants could be indirect due to defects in thalamocortical development evoked by ephrin A5 deficiency. However, we observed no gross alterations in the growth of L1-positive thalamic fibers during the timecourse of cortical neurogenesis in ephrin A5 mutants as compared with wild types (supplementary material Fig. S5C,D) (Fukuda et al., 1997). Moreover, thalamic explant cultures of wild-type and ephrin A5 knockout thalami (E14.5+2 days *in vitro*) did not reveal any differences in the axonal outgrowth index, which is defined as the ratio between the area of the whole explant and the area of the explant without axons (supplementary material Fig. S5E-G). This suggests a direct action of ephrin A5-expressing thalamic axons on EphA4-expressing cortical progenitors, rather than any indirect effect evoked by alterations of thalamic axonal projections due to ephrin A5 deficiency.

To show that ephrin A5 is expressed in thalamic axons and to circumvent the lack of specific antibodies for ephrin A5, we first applied Alexa 488-labeled recombinant EphA3-Fc protein to thalamic explant cultures prior to fixation in order to visualize ephrin A ligands, according to previous studies (Zimmer et al., 2011). As illustrated in Fig. 5A-D, we detected EphA3-Fc binding sites along βIII-tubulin-labeled thalamic axons indicating ephrin A ligand expression. Consistent with region-specific thalamic ephrin A5 expression (Fig. 4A-C), not all thalamic explants revealed EphA3-Fc binding sites (Fig. 5N,O). This excludes nonspecific labeling by the Alexa 488-conjugated anti-human IgG antibody used for detection of EphA3-Fc binding sites. Axonal mRNA localization and protein synthesis have already been described (Jung et al., 2012). To investigate whether ephrin A5 transcripts, in particular, can be identified in thalamic axons, we manually isolated axonal parts of thalamic explants (Fig. 5E-G) and performed RT-PCR. As a housekeeping gene we used β-actin (*Actb*), which was detected in axonal compartments but not in the negative controls. Indeed, we identified ephrin A5 transcripts in samples of thalamic axons (Fig. 5H). These data suggest that exogenous ephrin A5 ligands are imported into the cortex by thalamic axons.

Thalamocortical axons reach the cortex at E13.5

Auladell et al. (2000) provided evidence that thalamic afferents reach the cortex as early as E13. As L1 was used in other studies to label thalamocortical axons (Fukuda et al., 1997; Ohyama et al., 2004; Demyanenko et al., 2011), we performed immunohistochemical staining of L1 at E13.5, E14.5 and E16.5. Fibers positive for L1 were detected in the lateral cortex at E13.5, becoming increasingly evident with progressing developmental stages (Fig. 5I-K; supplementary material Fig. S5C). However, L1 is also expressed by early cortical projection neurons (Espinosa and Stryker, 2012). For this, we performed anterograde labeling of thalamic axons with the lipophilic dialkylaminostyryl dye (DiA) as an alternative approach. Labeling in living tissue is 6 mm/day faster than in fixed tissue (0.2-0.6 mm/day) due to active dye transport (Lukas et al., 1998). Thus, we injected DiA into the thalamus of freshly prepared brains at E13.5, which were then kept in culture for 10 h. After fixation, the tissue was stored for 7 days at 37°C to ensure complete axonal labeling. In agreement with Auladell et al. (2000), we observed DiA-positive thalamic fibers reaching the cortex at E13.5 (Fig. 5L,M). These data indicate that the arrival of the first thalamocortical fibers is coincident with the alterations that we observe in the dorsolateral cortex of E13.5 ephrin A5-deficient mice (Figs 1 and 2; supplementary material Figs S1-S3).

Development (2015) 142, 140-150 doi:10.1242/dev.104927

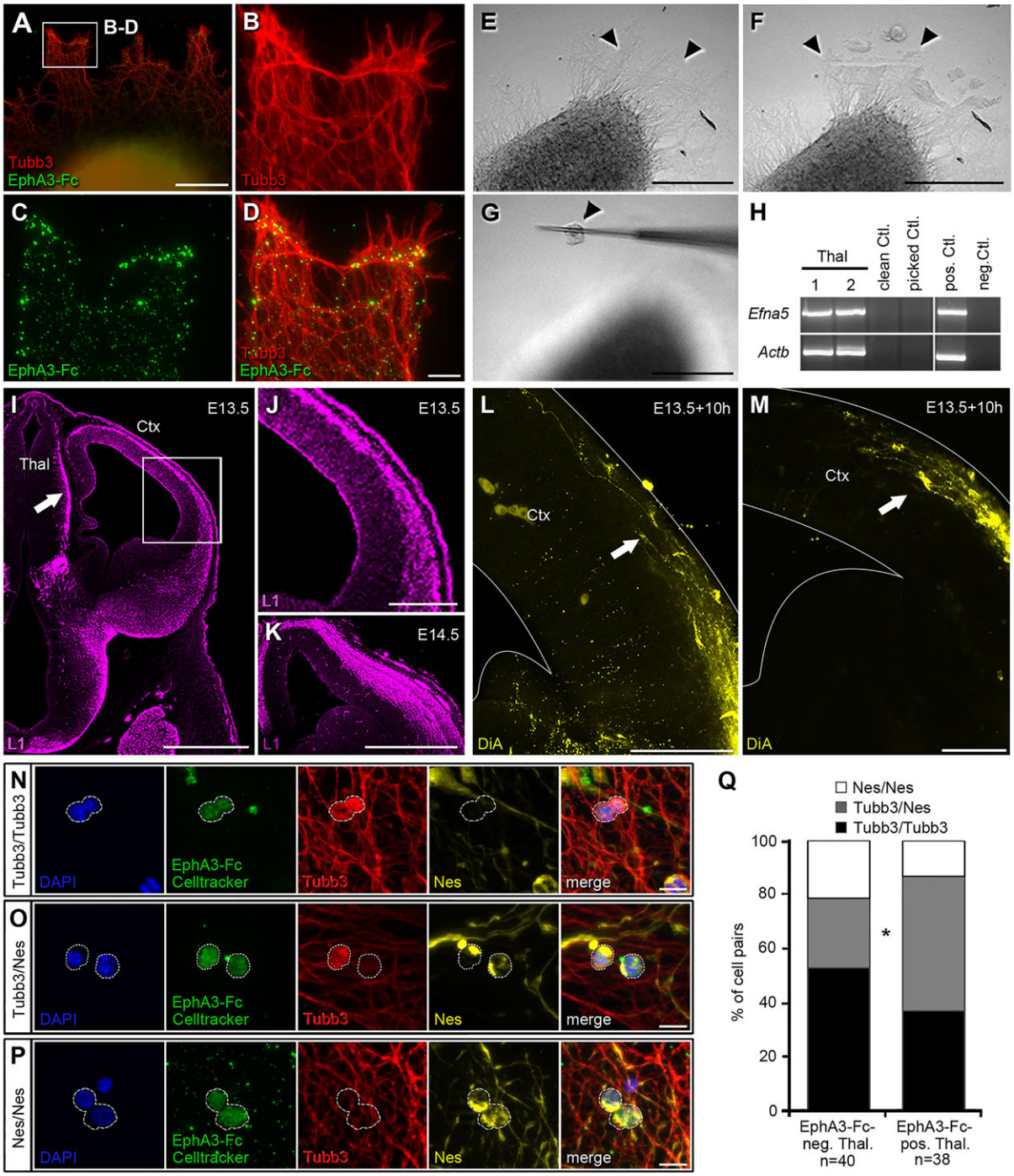

Fig. 5. Evidence for a regulation of cortical progenitors by ephrin A5 expressing thalamic axons. (A-D) Axons of thalamic explants (E14.5+1div) express ephrin A ligands as revealed by EphA3-Fc binding sites. (A) Thalamic explants were treated with EphA3-Fc prior to immunostaining for βIII-tubulin (Tubb3). The boxed region is magnified in B-D. (B) Immunostaining against βIII-tubulin. (C) EphA3-Fc binding sites visualized with an Alexa 488-labeled anti-Fc antibody. (D) Overlay of B and C. (E-H) Isolated axonal compartments from thalamic explants without soma contamination (E14.5+1div) (E-G; arrowheads indicate isolated axons) contained ephrin A5 transcripts (*Efna5*, 292 bp fragment) as revealed by RT-PCR (H); the housekeeping gene β-actin (*Actb*) provided a positive control. Single-cell libraries of preoptic area-derived cells and 3′-enriched cDNA libaries generated from E14.5/E16.5 embryonic brain tissue served as positive controls (pos. Ctl.); the negative control (neg. Ctl.) lacked cDNA. 1 and 2 refer to the axonal samples. Clean Ctl. and picked Ctl. refer to control conditions in which freshly prepared isolation buffer (clean control) and isolation buffer of the explants after axon isolation (picked control) were used as templates for cDNA synthesis to check for potential RNA contamination. (I-K) L1 immunostaining in coronal brain sections at E13.5 (I,J) and E14.5 (K). (I,J) At E13.5, L1 signals were detected in the thalamic mantle zone (arrow) and L1-positive fibers were observed growing through the basal telencephalon and entering the cortex (boxed region is magnified in J), which was even more evident at E14.5 (K). (L,M) DiA injections into the thalamus of whole brain cultures revealed DiA-stained fibers entering the cortex (E13.5+10 h). Arrows indicate thalamocortical fibers. (N-Q) Cell Tracker Green-labeled E13.5 single cortical cells co-cultured with either EphA3-Fc-negative (N,O) or EphA3-Fc-positive (P) E13.5 thalamic explants for 24 h and labeled by nestin/βIII-tubulin staining. Cell Tracker Green and clustered EphA3-Fc/Alexa 488 is shown in green. Cell pairs are outlined. (Q) Quantification of the proportion of cell pairs shows an increased proportion of βIII-tubulin/nestin-positive cell pairs (*P<0.05, Student's t-test) in response to EphA3-positive versus EphA3-negative thalamic axons (n refers to cell pairs; four different experiments). Ctx, cortex; Thal, thalamus. Scale bars: 500 µm in I,K; 200 µm in J; 100 µm in A,E-G,L,M; 10 µm in D,N-P.

Development (2015) 142, 140-150 doi:10.1242/dev.104927

Evidence for subcortical regulation of cortical progenitors by ephrin A ligand-expressing thalamocortical axons

The data described so far showed that ephrin A5-EphA4 interactions are involved in the regulation of cortical progenitors. As ephrin A5 was not detected in cortical cells but in the thalamus and thalamic axons, we hypothesize an exogenous regulation of cortical precursors by thalamic afferents. To address whether ephrin A-expressing thalamic axons affect the proliferation of cortical precursors, we performed a modified pair-cell assay in the presence of ephrin A ligand-positive or -negative thalamic axons. We co-cultured E13.5 thalamic explants and dissociated cortical cells (E13.5) labeled with Cell Tracker Green at clonal density. The ephrin A ligand-expressing thalamic axons were identified by binding of recombinant EphA3-Fc clustered with an Alexa 488-labeled anti-human IgG antibody, as EphA3 represents a high-affinity receptor for ephrin A ligands but does not interact with ephrin B ligands, in contrast to EphA4 (Fig. 5C,P). We determined the number of cell pairs localized within the area covered by thalamic axons around the explants that consisted of either two nestin-positive progenitors, two βIII-tubulin-positive postmitotic neurons, or mixed pairs composed of a nestin-positive cell and a βIII-tubulin-expressing cell (Fig. 5N-P). We detected a significant increase in the proportion of the mixed nestin/βIII-tubulin-positive combination accompanied by a decrease in βIII-tubulin-positive cell pairs and nestin-positive cell pairs in the presence of EphA3-Fc-positive axonal fibers as compared with EphA3-Fc-negative explants (Fig. 5Q). This is reminiscent of what was found for E13.5 cell pairs stimulated with recombinant ephrin A5-Fc (Fig. 2G). These *in vitro* data suggest that ephrin A-expressing thalamic fibers influence the proliferation and differentiation of cortical progenitors.

Thalamic fibers invade the developing cortex along the IMZ and upper SVZ (Auladell et al., 2000), whereas cortical progenitors reside in the VZ and SVZ. As EphA4 expression was observed along the radial processes of cortical progenitors, this scaffold might enable contact-dependent ephrin A5/EphA4 signaling between growing thalamic axons and neuronal precursors. To address this, we placed ephrin A5-Fc-coated or control Fc-coated protein-A-agarose beads in the CP/IMZ of organotypic coronal slice cultures of E14.5 ephrin A5 knockout brains. After 2 days *in vitro* we performed immunostaining against Tbr2, to investigate whether ectopic ephrin A5-Fc influences IPC numbers in ephrin A5-deficient cortices. This revealed an increase in Tbr2-positive cells in response to the ephrin A5-Fc-coated beads compared with the control after 2 days *in vitro* (supplementary material Fig. S5H-J). Thus, ectopically applied ephrin A5-Fc outside of the proliferative zones affects IPC production by regulating the division mode of RGCs. As we observed elevated levels of Tbr2-expressing cells when placing the ephrin A5-Fc-coated beads at E14.5+2 days *in vitro* into slices of ephrin A5-deficient brains, this can be regarded as a partial rescue of the IPC reduction observed in E16.5 knockout mice (Fig. 2).

Taken together, these data suggest that extra-cortical ephrin A5 ligands imported by invading thalamic axons regulate the proliferation and differentiation of cortical progenitors by activating EphA4 forward signaling and thereby the laminar organization of the cerebral cortex.

DISCUSSION

In this study, we provide evidence for the extra-cortical regulation of RGC division, regulating proper IPC levels at early and late stages of cortical neurogenesis by thalamic axons via ephrinA5/EphA4 signaling, thereby controlling the neuronal output fated for the deep and upper cortical layers.

The role of ephrins in the regulation of cortical progenitors

Control of cortical proliferation by the paracrine activation of Eph receptors was reported previously (Qiu et al., 2008; North et al., 2009). Here, we describe a contribution of ephrin A5 to the EphA4-dependent control of cortical progenitors. Interestingly, EphA4 has already been shown to regulate cortical progenitor proliferation; EphA4 overexpression enlarges the progenitor pool, whereas reduced EphA4 receptor forward signaling results in fewer mitotically active cells mediated by ephrin B1-EphA4 interactions (North et al., 2009).

Changes in adult cortical layers in ephrin A5-deficient mice correlate with altered IPC levels at embryonic stages

IPCs represent an intermediate stage from RGCs to neurons (Gotz and Huttner, 2005; Franco and Muller, 2013). Upon generation from RGCs in the VZ, IPCs translocate to the SVZ, where they undergo symmetric proliferative and neurogenic divisions (Attardo et al., 2008; Noctor et al., 2008). Even if IPCs are restricted in their proliferative potential, they expand the pool of neurogenic progenitors (Haubensak et al., 2004; Noctor et al., 2004) and contribute to all cortical layers (Smart, 1973; Haubensak et al., 2004; Attardo et al., 2008; Farkas et al., 2008; Sessa et al., 2008; Kowalczyk et al., 2009; Vasistha et al., 2014). It has even been suggested that the majority of cortical projection neurons derive from IPCs, whereas only ∼10% seem to be generated directly from RGCs (Attardo et al., 2008; Sessa et al., 2008; Kowalczyk et al., 2009). In support of this, we observed distinct changes in IPC numbers that concur with the neuronal output at early and late stages of neurogenesis in ephrin A5-deficient embryos and the altered thickness of infra- and supragranular adult cortical layers.

Our observations, including alterations in the RGC cleavage plane (Fig. 2A-C) and augmented IPC numbers in regions that represent the VZ (Fig. 2H-J), point to an ephrin A5 deficiency-induced shift in RGC division towards an elevated IPC production at E13.5. Furthermore, the increase in the number of both IPCs and postmitotic neurons in E13.5 ephrin A5-deficient cortices is in contradiction with the elevation of self-amplifying basally dividing cells observed after forced Insm1 expression, which occurs at the expense of neuronal production (Farkas et al., 2008). For this, an increase in proliferative basal cell division seems unlikely.

In contrast to IPCs, which showed significantly higher cell numbers in most of the regions of the E13.5 cortex, the slight increase in Pax6-positive cells was restricted to the upper segments, in which the majority of the Tbr2-positive IPCs are located. Thus, these cells could represent differentiating IPCs, which still express Pax6 consistent with the observation of Englund et al. (2005), thus revealing cells co-expressing both markers.

As the genetic ablation of ephrin B1 leads to premature neurogenesis and loss of cortical progenitors (Qiu et al., 2008), the switch towards decreased levels of IPCs at E16.5 and E18.5 might result from precocious augmentation at the subsequent expense of IPCs. Another possible scenario to explain the reduced IPC numbers is a reciprocal effect on the RGC division mode at E16.5 as compared with E13.5 mediated by distinct intracellular signaling molecules that evoke differential effects induced by the same ligand-receptor interaction at certain developmental stages. For ephrin A5-induced EphA4 receptor activation, a switch in the cellular response that is dependent on Src family kinase activity has already been shown (Zimmer et al., 2007).

Development (2015) 142, 140-150 doi:10.1242/dev.104927

Exogenous regulation of cortical progenitor cell fate by thalamic afferents

Here, we provide evidence for an extra-cortical regulation of neuronal precursors by thalamic afferents expressing ephrin A5. As we did not detect ephrin A5 in cortical progenitors or postmitotic neurons, consistent with previous reports (North et al., 2009; Deschamps et al., 2010), a paracrine signaling of cortical precursors (Qiu et al., 2008; North et al., 2009) or feedback signaling of CP neurons back to progenitors (Seuntjens et al., 2009; Parthasarathy et al., 2014; Toma et al., 2014) seems unlikely. However, we identified ephrin A5 transcripts in the developing thalamus and thalamic axons. Axonal mRNA transport, localization and translation, as has also been described for ephrins, serves to provide a rapid response to guidance cues during axonal growth and synapse formation (Jung et al., 2012).

Thalamic afferents have been shown to contribute to cortical arealization (Rakic, 1988; Dehay et al., 1996a,b), to influence the survival and identity of postmitotic cortical neurons (Zhou et al., 2010; Sato et al., 2012; Li et al., 2013) and to affect cortical progenitor proliferation *in vitro* by a diffusible factor (Dehay et al., 2001). Here, we follow the idea of thalamic regulation of cortical progenitors by suggesting that thalamic ephrin A5 interacts with EphA4 receptors of RGCs to regulate the proper levels of IPCs. The radial processes of RGCs provide the structural scaffold for local interactions of membrane-bound EphA4 receptors with ephrin A5 ligands expressed by thalamic afferents, growing along the upper SVZ and IMZ (Auladell et al., 2000). In support of this, we observed increased IPC numbers in cortical slice cultures of ephrin A5-deficient mice in response to ephrin A5-Fc-coated protein-A-agarose beads placed in the CP/IMZ.

The idea of afferents affecting the proliferation of telencephalic structures was proposed by Gong and Shipley (1995), who showed that pioneer olfactory axons modulate the cell cycle kinetics of olfactory bulb precursors. A thalamic influence on cortical proliferation was further shown for cortical progenitors in ferrets, affecting the tangential expansion of the cortex (Reillo et al., 2011). In *Celsr3*/*Dlx* mutant mice lacking thalamocortical and corticothalamic connections, the thalamic impact on cortical neurogenesis is suggested to be rather subtle, based on laminar architecture and BrdU birthdating analysis in adults. Interestingly, BrdU labeling of the upper cortical layers in the *Celsr3*/*Dlx* mutant mice revealed a shift towards the pial surface and a reduction in the radial extension of the BrdU-labeled upper layer neurons (Zhou et al., 2010), similar to our observation in ephrin A5 knockout mice (supplementary material Fig. S1F-H). However, the subtle defects observed in *Celsr3*/*Dlx* mutant and ephrin A5-deficient mice indicate an involvement of thalamic axons in the fine-tuning of cortical neurogenesis.

Thalamocortical projections have been reported to arrive in the cerebral cortex prior to the generation of the majority of cortical neurons (Shatz and Luskin, 1986; Auladell et al., 2000). Deep layer neurons are generated between E12.5 and E14.5, whereas upper layer neurons are born from E15.5-E18.5 (Polleux et al., 1997). Auladell et al. (2000) describes the first thalamocortical axons as arriving at E13 in the murine dorsolateral cortex. Consistently, by DiA labeling in living brain cultures we traced fibers in the dorsolateral cortex labeling the E13.5 thalamus, suggesting that thalamic ephrin A5 instructs cortical progenitors from E13.5 on. However, in the context of the effects on neuronal numbers that we observed at E13.5, we cannot discount the possible influence of other sources of ephrin A5, the detection of which was beyond the scope of this study.

Ephrin A5-EphA receptor interactions regulate the topography of different thalamocortical projections at later stages (Donoghue and Rakic, 1999; Šestan et al., 2001; Bolz et al., 2004). As we did not observe gross alterations in thalamic axonal growth between wild type and ephrin A5 knockouts we suggest a direct influence of ephrin A5 on cortical progenitors.

In conclusion, we propose an influence of invading thalamic axons on the balance of basal cortical progenitors, thereby regulating cortical neurogenesis via ephrin A5-EphA4 interactions.

MATERIALS AND METHODS

Animals

Time-staged embryos (E1 being the day of insemination) and adult animals (P37) of the ephrin A5 knockout (Knoll et al., 2001), EphA4 PLAP mice (Leighton et al., 2001) and wild-type (C57/BL6) mice, bred and maintained under standard conditions (food and water *ad libitum*, 12-h light/dark cycle), were used. All animal procedures were performed in accordance with guidelines for the care and use of laboratory animals of the Friedrich Schiller University, Jena, and the University Hospital Jena, Germany.

Preparation of adult and embryonic brains

For the preparation of adult brains, mice were transcardially perfused with PBS (pH 7.4) and 4% paraformaldehyde (PFA) solution (pH7.4) and post-fixed overnight in 4% PFA followed by treatment with 10% and 30% sucrose in PBS overnight. For the preparation of time-staged embryonic brains, mice were deeply anesthetized with 10% chloralhydrate in PBS (pH 7.4) and prepared embryonic brains were used fresh or fixed for 5 h in 4% PFA followed by treatment with 10% and 30% sucrose overnight.

Preparation of organotypic slice cultures, dissociated cortical cells and thalamic explants

For organotypic slice preparation the protocol described by Zimmer et al. (2011) was used. The preparation of dissociated cells was performed according to Zimmer et al. (2007). Cells were seeded at a density of 300 cells/mm^2 for immunohistochemistry and stimulation experiments and at 150 cells/mm^2 for the DAB TUNEL-based apoptosis detection assay (see supplementary methods). Thalamic explants were prepared according to Ruediger et al. (2013).

Pair-cell assay

E13.5 cortical cells plated at clonal density in DMEM/F12 supplemented with 10% FBS, 0.4% methyl cellulose, 72 mM glucose, 100 U/ml penicillin, 100 µg/ml streptomycin and 0.4 mM L-glutamine were incubated for 24 h *in vitro*, supplementing the medium with either 5 µg/ml ephrin A5-Fc (R&D Systems) or Fc protein as control (Rockland Immunochemicals) clustered with 50 µg/ml anti-human IgG antibody (Alexis Biochemicals). Cell pair identity was determined after 24 h by immunostaining for nestin and βIII-tubulin. We included only cell pairs in our analysis that showed staining of both cells.

Co-culture of thalamic explants with single cortical cells

Dissociated cortical cells were treated with Cell Tracker Green (Life Technologies) and washed before adding to explants at clonal density on coverslips coated with 19 µg/ml laminine and 5 µg/ml poly-L-lysine (Gibco) in DMEM/F12 supplemented with 10% FBS, 0.4% methyl cellulose, 72 mM glucose, 100 U/ml penicillin, 100 µg/ml streptomycin and 0.4 mM L-glutamine. After 24 h at 37°C and 5% CO_2, 5 µg/ml EphA3-Fc (R&D Systems) pre-clustered with 50 µg/ml Alexa 488-conjugated anti-human IgG (Alexis Biochemicals) was added for 30 min at 37°C. After fixation in 4% PFA in PBS for 30 min, cell pair identity was determined by immunostaining against nestin and βIII-tubulin.

Stimulation with recombinant proteins

Stimulation of dissociated cells and organotypic brain slices with 5 µg/ml recombinant ephrin A5-Fc or EphA3-Fc (R&D Systems) clustered with 50 µg/ml anti-human IgG Alexa 488 (Chemicon) was performed for 3 h at

Development (2015) 142, 140-150 doi:10.1242/dev.104927

37°C and 5% CO_2. For the application of either ephrin A5-Fc-coated or Fc-protein-coated protein-A-agarose (Santa Cruz Biotechnology), beads were treated overnight with 5 µg/ml recombinant ephrin A5-Fc or Fc at 4°C on a shaker.

DiA injections in brain cultures

DiA (in 25% DMSO, 25% ethanol, 50% DMEM/F12) was pressure injected with an extended glass capillary into the embryonic thalamus of E13.5 brains. After washing in Krebs buffer, brains were incubated in 3 ml culture medium (DMEM/F12 supplemented with 20 mM glucose, 100 U/ml penicillin, 100 µg/ml streptomycin, 55 mM mercaptoethanol) on an orbital shaker (50 rpm). After 10 h incubation at 37°C and 5% CO_2, brains were fixed in 4% PFA in PBS (pH 7.4) and stored at 37°C for 7 days. Brains were coronally dissected into 300 µm slices.

Histochemistry

For immunohistochemistry, fixed embryonic brains (5 h in 4% PFA in PBS) or single cells (15 min in 4% PFA in PBS) were used. Histochemistry is performed as described by Zimmer et al. (2011). Primary antibodies were applied overnight, secondary antibodies for 2 h. For further details, see the supplementary methods.

In situ hybridization

In situ hybridizations were performed as described by Zimmer et al. (2011) using digoxigenin-labeled riboprobes spanning the sequence 75-761 for *Epha4* (accession number 007936) and 106-637 for *Efna5* (accession number 010109). Riboprobes were obtained by *in vitro* transcription using DIG-11-UTP (Roche) from cDNA fragments cloned in pBluescript I KS (Stratagene).

PCR

The protocol for global cDNA synthesis was from Iscove et al. (2002) with the modifications presented in the supplementary methods. Preparation of cortical tissue for PCR and details of single-cell RT-PCR and RT-PCR of thalamic axons are described in the supplementary methods.

Imaging and analysis

A detailed description of the image analyses performed, including quantification of cortical progenitors and characterization of cell pairs, measurements of radial extension of cortical structures/layers, analysis of the *Insm1* signal and determination of division angles, together with statistical considerations, is presented in the supplementary methods.

Acknowledgements

We thank Christine Raue for excellent technical assistance and Sandra Clemens for animal breeding (Institut für Allgemeine Zoologie, Friedrich-Schiller Universität Jena, Germany). We thank Hans Zempel for correcting the manuscript. The L1 (rat) antibody developed by P. H. Patterson was obtained from the Developmental Studies Hybridoma Bank, created by the NICHD of the NIH and maintained at the University of Iowa, Department of Biology, Iowa City, IA, USA.

Competing interests

The authors declare no competing financial interests.

Author contributions

K.G. performed experiments and data analysis, assisted in the conceptual design of experiments, corrected the manuscript and prepared figure illustrations. D.P. performed experiments and data analysis, figure illustration and corrected the manuscript. J.S. performed experiments, data analysis and assisted in figure illustration. M.K. performed experiments, data analysis and figure illustration. C.A.H. provided support and assisted in writing the manuscript. J.B. initiated this study, contributed the conceptual design of the project and corrected the manuscript. G.Z. performed experiments and data analysis, contributed the conceptual design of the project and wrote the manuscript.

Funding

This project was funded by the Deutsche Forschungsgemeinschaft (DFG) [ZI-1224/2-1 and ZI-1224/4-1] and by the Else Kröner–Fresenius-Stiftung (EKFS) [213-A253].

Supplementary material

Supplementary material available online at
http://dev.biologists.org/lookup/suppl/doi:10.1242/dev.104927/-/DC1

References

Asami, M., Pilz, G. A., Ninkovic, J., Godinho, L., Schroeder, T., Huttner, W. B. and Gotz, M. (2011). The role of Pax6 in regulating the orientation and mode of cell division of progenitors in the mouse cerebral cortex. *Development* **138**, 5067-5078.

Attardo, A., Calegari, F., Haubensak, W., Wilsch-Bräuninger, M. and Huttner, W. B. (2008). Live imaging at the onset of cortical neurogenesis reveals differential appearance of the neuronal phenotype in apical versus basal progenitor progeny. *PLoS ONE* **3**, e2388.

Auladell, C., Pérez-Sust, P., Supèr, H. and Soriano, E. (2000). The early development of thalamocortical and corticothalamic projections in the mouse. *Anat. Embryol. (Berl.)* **201**, 169-179.

Bolz, J., Uziel, D., Mühlfriedel, S., Güllmar, A., Peuckert, C., Zarbalis, K., Wurst, W., Torii, M. and Levitt, P. (2004). Multiple roles of ephrins during the formation of thalamocortical projections: maps and more. *J. Neurobiol.* **59**, 82-94.

Chenn, A. and McConnell, S. K. (1995). Cleavage orientation and the asymmetric inheritance of Notch1 immunoreactivity in mammalian neurogenesis. *Cell* **82**, 631-641.

Davis, S., Gale, N. W., Aldrich, T. H., Maisonpierre, P. C., Lhotak, V., Pawson, T., Goldfarb, M. and Yancopoulos, G. D. (1994). Ligands for EPH-related receptor tyrosine kinases that require membrane attachment or clustering for activity. *Science* **266**, 816-819.

Dehay, C., Giroud, P., Berland, M., Killackey, H. P. and Kennedy, H. (1996a). Phenotypic characterisation of respecified visual cortex subsequent to prenatal enucleation in the monkey: development of acetylcholinesterase and cytochrome oxidase patterns. *J. Comp. Neurol.* **376**, 386-402.

Dehay, C., Giroud, P., Berland, M., Killackey, H. and Kennedy, H. (1996b). Contribution of thalamic input to the specification of cytoarchitectonic cortical fields in the primate: effects of bilateral enucleation in the fetal monkey on the boundaries, dimensions, and gyrification of striate and extrastriate cortex. *J. Comp. Neurol.* **367**, 70-89.

Dehay, C., Savatier, P., Cortay, V. and Kennedy, H. (2001). Cell-cycle kinetics of neocortical precursors are influenced by embryonic thalamic axons. *J. Neurosci.* **21**, 201-214.

Demyanenko, G. P., Siesser, P. F., Wright, A. G., Brennaman, L. H., Bartsch, U., Schachner, M. and Maness, P. F. (2011). L1 and CHL1 cooperate in thalamocortical axon targeting. *Cereb. Cortex* **21**, 401-412.

Depaepe, V., Suarez-Gonzalez, N., Dufour, A., Passante, L., Gorski, J. A., Jones, K. R., Ledent, C. and Vanderhaeghen, P. (2005). Ephrin signalling controls brain size by regulating apoptosis of neural progenitors. *Nature* **435**, 1244-1250.

Deschamps, C., Morel, M., Janet, T., Page, G., Jaber, M., Gaillard, A. and Prestoz, L. (2010). EphrinA5 protein distribution in the developing mouse brain. *BMC Neurosci.* **11**, 105.

Donoghue, M. J. and Rakic, P. (1999). Molecular evidence for the early specification of presumptive functional domains in the embryonic primate cerebral cortex. *J. Neurosci.* **19**, 5967-5979.

Drescher, U., Bonhoeffer, F. and Müller, B. K. (1997). The Eph family in retinal axon guidance. *Curr. Opin. Neurobiol.* **7**, 75-80.

Englund, C., Fink, A., Lau, C., Pham, D., Daza, R. A. M., Bulfone, A., Kowalczyk, T. and Hevner, R. F. (2005). Pax6, Tbr2, and Tbr1 are expressed sequentially by radial glia, intermediate progenitor cells, and postmitotic neurons in developing neocortex. *J. Neurosci.* **25**, 247-251.

Espinosa, J. S. and Stryker, M. P. (2012). Development and plasticity of the primary visual cortex. *Neuron* **75**, 230-249.

Farkas, L. M., Haffner, C., Giger, T., Khaitovich, P., Nowick, K., Birchmeier, C., Pääbo, S. and Huttner, W. B. (2008). Insulinoma-associated 1 has a panneurogenic role and promotes the generation and expansion of basal progenitors in the developing mouse neocortex. *Neuron* **60**, 40-55.

Fish, J. L., Kosodo, Y., Enard, W., Paabo, S. and Huttner, W. B. (2006). Aspm specifically maintains symmetric proliferative divisions of neuroepithelial cells. *Proc. Natl. Acad. Sci. USA* **103**, 10438-10443.

Flanagan, J. G. and Vanderhaeghen, P. (1998). The ephrins and Eph receptors in neural development. *Annu. Rev. Neurosci.* **21**, 309-345.

Franco, S. J. and Müller, U. (2013). Shaping our minds: stem and progenitor cell diversity in the mammalian neocortex. *Neuron* **77**, 19-34.

Frantz, G. D. and McConnell, S. K. (1996). Restriction of late cerebral cortical progenitors to an upper-layer fate. *Neuron* **17**, 55-61.

Fujiwara, T., Kubo, T., Koyama, Y., Tomita, K., Yano, K., Tohyama, M. and Hosokawa, K. (2008). mRNA expression changes of slit proteins following peripheral nerve injury in the rat model. *J. Chem. Neuroanat.* **36**, 170-176.

Fukuda, T., Kawano, H., Ohyama, K., Li, H.-P., Takeda, Y., Oohira, A. and Kawamura, K. (1997). Immunohistochemical localization of neurocan and L1 in the formation of thalamocortical pathway of developing rats. *J. Comp. Neurol.* **382**, 141-152.

Gauthier-Fisher, A., Lin, D. C., Greeve, M., Kaplan, D. R., Rottapel, R. and Miller, F. D. (2009). Lfc and Tctex-1 regulate the genesis of neurons from cortical precursor cells. *Nat. Neurosci.* **12**, 735-744.
Gong, Q. and Shipley, M. T. (1995). Evidence that pioneer olfactory axons regulate telencephalon cell cycle kinetics to induce the formation of the olfactory bulb. *Neuron* **14**, 91-101.
Götz, M. and Huttner, W. B. (2005). The cell biology of neurogenesis. *Nat. Rev. Mol. Cell Biol.* **6**, 777-788.
Götz, M., Stoykova, A. and Gruss, P. (1998). Pax6 controls radial glia differentiation in the cerebral cortex. *Neuron* **21**, 1031-1044.
Haubensak, W., Attardo, A., Denk, W. and Huttner, W. B. (2004). Neurons arise in the basal neuroepithelium of the early mammalian telencephalon: a major site of neurogenesis. *Proc. Natl. Acad. Sci. USA* **101**, 3196-3201.
Iscove, N. N., Barbara, M., Gu, M., Gibson, M., Modi, C. and Winegarden, N. (2002). Representation is faithfully preserved in global cDNA amplified exponentially from sub-picogram quantities of mRNA. *Nat. Biotechnol.* **20**, 940-943.
Jung, H., Yoon, B. C. and Holt, C. E. (2012). Axonal mRNA localization and local protein synthesis in nervous system assembly, maintenance and repair. *Nat. Rev. Neurosci.* **13**, 308-324.
Knöll, B., Isenmann, S., Kilic, E., Walkenhorst, J., Engel, S., Wehinger, J., Bähr, M. and Drescher, U. (2001). Graded expression patterns of ephrin-As in the superior colliculus after lesion of the adult mouse optic nerve. *Mech. Dev.* **106**, 119-127.
Kolk, S. M., Whitman, M. C., Yun, M. E., Shete, P. and Donoghue, M. J. (2005). A unique subpopulation of Tbr1-expressing deep layer neurons in the developing cerebral cortex. *Mol. Cell. Neurosci.* **30**, 538-551.
Kowalczyk, T., Pontious, A., Englund, C., Daza, R. A. M., Bedogni, F., Hodge, R., Attardo, A., Bell, C., Huttner, W. B. and Hevner, R. F. (2009). Intermediate neuronal progenitors (basal progenitors) produce pyramidal-projection neurons for all layers of cerebral cortex. *Cereb. Cortex* **19**, 2439-2450.
Kriegstein, A. R. and Götz, M. (2003). Radial glia diversity: a matter of cell fate. *Glia* **43**, 37-43.
Lehtinen, M. K. and Walsh, C. A. (2011). Neurogenesis at the brain-cerebrospinal fluid interface. *Annu. Rev. Cell Dev. Biol.* **27**, 653-679.
Leighton, P. A., Mitchell, K. J., Goodrich, L. V., Lu, X., Pinson, K., Scherz, P., Skarnes, W. C. and Tessier-Lavigne, M. (2001). Defining brain wiring patterns and mechanisms through gene trapping in mice. *Nature* **410**, 174-179.
Li, H., Fertuzinhos, S., Mohns, E., Hnasko, T. S., Verhage, M., Edwards, R., Šestan, N. and Crair, M. C. (2013). Laminar and columnar development of barrel cortex relies on thalamocortical neurotransmission. *Neuron* **79**, 970-986.
Lukas, J.-R., Aigner, M., Denk, M., Heinzl, H., Burian, M. and Mayr, R. (1998). Carbocyanine postmortem neuronal tracing: influence of different parameters on tracing distance and combination with immunocytochemistry. *J. Histochem. Cytochem.* **46**, 901-910.
Nieto, M., Monuki, E. S., Tang, H., Imitola, J., Haubst, N., Khoury, S. J., Cunningham, J., Gotz, M. and Walsh, C. A. (2004). Expression of Cux-1 and Cux-2 in the subventricular zone and upper layers II-IV of the cerebral cortex. *J. Comp. Neurol.* **479**, 168-180.
Noctor, S. C., Martínez-Cerdeño, V., Ivic, L. and Kriegstein, A. R. (2004). Cortical neurons arise in symmetric and asymmetric division zones and migrate through specific phases. *Nat. Neurosci.* **7**, 136-144.
Noctor, S. C., Martínez-Cerdeño, V. and Kriegstein, A. R. (2008). Distinct behaviors of neural stem and progenitor cells underlie cortical neurogenesis. *J. Comp. Neurol.* **508**, 28-44.
North, H. A., Zhao, X., Kolk, S. M., Clifford, M. A., Ziskind, D. M. and Donoghue, M. J. (2009). Promotion of proliferation in the developing cerebral cortex by EphA4 forward signaling. *Development* **136**, 2467-2476.
Ohyama, K., Tan-Takeuchi, K., Kutsche, M., Schachner, M., Uyemura, K. and Kawamura, K. (2004). Neural cell adhesion molecule L1 is required for fasciculation and routing of thalamocortical fibres and corticothalamic fibres. *Neurosci. Res.* **48**, 471-475.
Parthasarathy, S., Srivatsa, S., Nityanandam, A. and Tarabykin, V. (2014). Ntf3 acts downstream of Sip1 in cortical postmitotic neurons to control progenitor cell fate through feedback signaling. *Development* **141**, 3324-3330.
Polleux, F., Dehay, C. and Kennedy, H. (1997). The timetable of laminar neurogenesis contributes to the specification of cortical areas in mouse isocortex. *J. Comp. Neurol.* **385**, 95-116.
Pontious, A., Kowalczyk, T., Englund, C. and Hevner, R. F. (2008). Role of intermediate progenitor cells in cerebral cortex development. *Dev. Neurosci.* **30**, 24-32.
Qiu, R., Wang, X., Davy, A., Wu, C., Murai, K., Zhang, H., Flanagan, J. G., Soriano, P. and Lu, Q. (2008). Regulation of neural progenitor cell state by ephrin-B. *J. Cell Biol.* **181**, 973-983.
Rakic, P. (1988). Specification of cerebral cortical areas. *Science* **241**, 170-176.
Rakic, P. (1991). Experimental manipulation of cerebral cortical areas in primates. *Philos. Trans. R. Soc. Lond. B Biol. Sci.* **331**, 291-294.
Rakic, P., Ayoub, A. E., Breunig, J. J. and Dominguez, M. H. (2009). Decision by division: making cortical maps. *Trends Neurosci.* **32**, 291-301.
Rao, S. G., Williams, G. V. and Goldman-Rakic, P. S. (2000). Destruction and creation of spatial tuning by disinhibition: GABA(A) blockade of prefrontal cortical neurons engaged by working memory. *J. Neurosci.* **20**, 485-494.
Reillo, I., de Juan Romero, C., Garcia-Cabezas, M. A. and Borrell, V. (2011). A role for intermediate radial glia in the tangential expansion of the mammalian cerebral cortex. *Cereb. Cortex* **21**, 1674-1694.
Rosenbaum, J. N., Duggan, A. and García-Añoveros, J. (2011). Insm1 promotes the transition of olfactory progenitors from apical and proliferative to basal, terminally dividing and neuronogenic. *Neural Dev.* **6**, 6.
Rudolph, J., Zimmer, G., Steinecke, A., Barchmann, S. and Bolz, J. (2010). Ephrins guide migrating cortical interneurons in the basal telencephalon. *Cell Adh. Migr.* **4**, 400-408.
Ruediger, T., Zimmer, G., Barchmann, S., Castellani, V., Bagnard, D. and Bolz, J. (2013). Integration of opposing semaphorin guidance cues in cortical axons. *Cereb. Cortex* **23**, 604-614.
Sato, H., Fukutani, Y., Yamamoto, Y., Tatara, E., Takemoto, M., Shimamura, K. and Yamamoto, N. (2012). Thalamus-derived molecules promote survival and dendritic growth of developing cortical neurons. *J. Neurosci.* **32**, 15388-15402.
Sessa, A., Mao, C.-a., Hadjantonakis, A.-K., Klein, W. H. and Broccoli, V. (2008). Tbr2 directs conversion of radial glia into basal precursors and guides neuronal amplification by indirect neurogenesis in the developing neocortex. *Neuron* **60**, 56-69.
Šestan, N., Rakic, P. and Donoghue, M. J. (2001). Independent parcellation of the embryonic visual cortex and thalamus revealed by combinatorial Eph/ephrin gene expression. *Curr. Biol.* **11**, 39-43.
Seuntjens, E., Nityanandam, A., Miquelajauregui, A., Debruyn, J., Stryjewska, A., Goebbels, S., Nave, K.-A., Huylebroeck, D. and Tarabykin, V. (2009). Sip1 regulates sequential fate decisions by feedback signaling from postmitotic neurons to progenitors. *Nat. Neurosci.* **12**, 1373-1380.
Shatz, C. J. and Luskin, M. B. (1986). The relationship between the geniculocortical afferents and their cortical target cells during development of the cat's primary visual cortex. *J. Neurosci.* **6**, 3655-3668.
Siegenthaler, J. A. and Miller, M. W. (2008). Generation of Cajal-Retzius neurons in mouse forebrain is regulated by transforming growth factor beta-Fox signaling pathways. *Dev. Biol.* **313**, 35-46.
Smart, I. H. (1973). Proliferative characteristics of the ependymal layer during the early development of the mouse neocortex: a pilot study based on recording the number, location and plane of cleavage of mitotic figures. *J. Anat.* **116**, 67-91.
Tiberi, L., Vanderhaeghen, P. and van den Ameele, J. (2012). Cortical neurogenesis and morphogens: diversity of cues, sources and functions. *Curr. Opin. Cell Biol.* **24**, 269-276.
Toma, K., Kumamoto, T. and Hanashima, C. (2014). The timing of upper-layer neurogenesis is conferred by sequential derepression and negative feedback from deep-layer neurons. *J. Neurosci.* **34**, 13259-13276.
Uziel, D., Garcez, P., Lent, R., Peuckert, C., Niehage, R., Weth, F. and Bolz, J. (2006). Connecting thalamus and cortex: the role of ephrins. *Anat. Rec. A Discov. Mol. Cell. Evol. Biol.* **288A**, 135-142.
Vasistha, N. A., Garcia-Moreno, F., Arora, S., Cheung, A. F., Arnold, S. J., Robertson, E. J. and Molnar, Z. (2014). Cortical and clonal contribution of Tbr2 expressing progenitors in the developing mouse brain. *Cereb. Cortex* pii: bhu125 (in press).
Zhou, L., Gall, D., Qu, Y., Prigogine, C., Cheron, G., Tissir, F., Schiffmann, S. N. and Goffinet, A. M. (2010). Maturation of "neocortex isole" in vivo in mice. *J. Neurosci.* **30**, 7928-7939.
Zimmer, C., Tiveron, M.-C., Bodmer, R. and Cremer, H. (2004). Dynamics of Cux2 expression suggests that an early pool of SVZ precursors is fated to become upper cortical layer neurons. *Cereb. Cortex* **14**, 1408-1420.
Zimmer, G., Kastner, B., Weth, F. and Bolz, J. (2007). Multiple effects of ephrin-A5 on cortical neurons are mediated by SRC family kinases. *J. Neurosci.* **27**, 5643-5653.
Zimmer, G., Garcez, P., Rudolph, J., Niehage, R., Weth, F., Lent, R. and Bolz, J. (2008). Ephrin-A5 acts as a repulsive cue for migrating cortical interneurons. *Eur. J. Neurosci.* **28**, 62-73.
Zimmer, G., Rudolph, J., Landmann, J., Gerstmann, K., Steinecke, A., Gampe, C. and Bolz, J. (2011). Bidirectional ephrinB3/EphA4 signaling mediates the segregation of medial ganglionic eminence- and preoptic area-derived interneurons in the deep and superficial migratory stream. *J. Neurosci.* **31**, 18364-18380.

Supplementary Information

Supplementary Methods

Preparation of cortical tissue for PCR

The somatosensory cortex prepared from E14.5, P8 and P37 mice was collected in Trizol reagent (Invitrogen, Germany) and RNA was purified according to the manufacturer´s instructions. After DNase treatment (Thermo scientific, USA), limited reverse transcription was performed using the RevertAidTM H Minus M-MuLV Reverse Transkriptase (Thermo scientific, USA). PCR with sequence specific primer for *Efna5* and *β-actin* (*Actb*) was performed (*β-Actin* forw AGA GGG AAA TCG TGC G, *β-Actin* rev CAA TAG TGA TGA CCT GGC CGT, *Efna5* forw ATG TTG CAC GTG GAG ATG TTG AC, *Efna5* rev GCT ATA ATG TCA AAA GCA TCG CC).

DAB TUNEL based apoptosis detection assay

E14.5 cortical cells were either grown on ephrin A5-Fc-coated or Fc-control protein-coated coverslips in DMEM/F12 supplemented with 10% FBS, 100 U/ml penicillin, 100 µg/ml streptomycin, and 0.4 mM L-glutamine at 37°C and 5% CO_2 in a humid atmosphere. Coating of coverslips with recombinant 8 µg/ml ephrin A5-Fc or Fc was performed according to Zimmer et al. (2007). Cells were fixed after 5 hours and a DAB TUNEL based apoptosis detection assay (R&D systems, USA) was performed according to the manufacturer´s instructions. The percentage of DAB-stained cells was determined.

Histochemistry

For primary antibodies we applied: rabbit anti Aspm (gift from Prof. W.Huttner, MPI Dresden, Germany) 1:1000; rat anti BrdU (abcam, UK) 1:300, rabbit anti Calbindin (Swant, Switzerland) 1:1000, rabbit anti CDP (Cux2, Santa Cruz Biotechnology, USA) 1:200, rabbit anti EphA4 (Santa Cruz Biotechnology, USA) 1:100, rabbit anti Ki67 (Leica, Germany) 1:200, rabbit anti L1 (DSHB, USA) 1:100, mouse anti nestin (Millipore, USA) 1:500, mouse anti NeuN (Millipore, USA) 1:100, mouse anti Otx 1,2 (Chemicon, USA) 1:300, mouse anti Pax6 (Millipore, USA) 1:100, rabbit anti pTyr (PY350, Santa Cruz Biotechnology, USA) 1:50, rabbit anti Tbr1 (Abcam, UK) 1:400, rabbit anti Tbr2 (Abcam, UK) 1:500, and rabbit anti βIII-tubulin (Sigma, Germany) 1:300. Secondary antibodies: Cy2-conjugated anti-mouse IgG (Jackson,

USA) 1:500, Cy2-conjugated anti-rabbit IgG (Jackson, USA) 1:500, Cy3-conjugated anti rabbit IgG (Jackson, USA) 1:500 and Cy5-conjugated anti-mouse IgG (molecular probes, USA) 1:1000. For the Tbr2 immunostaining of organotypic slice cultures all washing steps were performed in PBS/0.2% Triton-X-100 for five times 20 minutes under orbital shaking (50 rpm). Sections were fixed in 4% PFA in PBS for 1.5 hours and blocked for 2 hours in 10% normal goat serum, 4% bovine serum albumine in PBS/0.2% Triton-X-100 prior to primary antibody treatment overnight and secondary antibody for 5 hours.

Single cell RT-PCR and RT-PCR of thalamic axons

Individual cells and thalamic axons were manually isolated under visual control using a micromanipulator and fire-polished borosilicate glass capillaries (outside-Ø 1 mm, wall thickness 0.13-0.22 mm; tip diameter 40 µm, Hilgenberg or Science products, Germany). Each cell was isolated using a fresh capillary and washed twice in fresh buffer (HBSS, free of Ca^{2+} and Mg^{2+}; 1% FBS) before transferred to a PCR vial containing 4.5 µl lysis & first strand buffer (50 mM Tris-HCl (pH 8.3); 75 mM KCl; 3 mM $MgCl_2$; 1 mM DTT; 0.5% (v/v) Igepal CA-630; 100 µg/ml acetylated BSA (Sigma-Aldrich, Germany); 10 µM each of dATP, dCTP, dGTP und dTTP; 3.5 nM SR-T_{24}-Primer (5'-GTTAACTCGAGAATTCT$_{24}$-3'); 0.04 U/µl *RiboLock™* RNase inhibitor (Fermentas, Germany); 0.03 U/µl *SuperaseIn™* RNase inhibitor (Ambion, USA) followed by subsequent freezing in liquid nitrogen. The protocol for global cDNA synthesis we applied here was adopted from Iscove et al. (2002) with modifications, including a limited reverse transcription prior to exponential amplification, leading to size-restricted and 3´enriched cDNA fragments. Qualitative evaluation of amplified cDNAs from single-cells and thalamic axons was done by PCR amplification using specific primers for relevant transcripts and *housekeeping* genes (*ActB* forward CAGCATTGCTTCTGTGTAAATTATG, *ActB* reverse GCACTTTTATTGGTCTCAAGTCAGT, *Pax6* forward CGGATCTGTGTTGCTCATGT, *Pax6* reverse CAACCTTTGGAAAACCAACA, *Tbr2* forward CCTGGTGGTGTTTTGTTGTG, *Tbr2* reverse AATCCAGCACCTTGAACGAC, *HuD (ELAVL4)* forward TGCACATTGAAGAGGCAAAC , *HuD (ELAVL4)* reverse TCCAAAAACCGAAAAGAGGA, *EfnA5* forward CTTTTGAAAATCGCCTCCAC, *EfnA5* reverse AGACAGACCTGCCCATTCAC, *EphA4* forward AAATCAAGCCGTTTCACCAC, *EphA4* reverse CGTCCCCTTCACAGATGAAT). As negative controls we used reaction products of "picked" controls, whereby the whole manual cell isolation procedure was performed without taking up a cell. As positive control, we used

cDNA libraries generated from single cell equivalent dilutions (10 pg) of E14.5/E16.5 RNA isolated from whole brain tissue to validate the functionality of the respective primer in the limited 3´cDNA libraries.

Imaging and detailed description of analysis

Fluorescent pictures were captured with a confocal laser scanning microscope TCS SP5 (Leica Microsystems, Germany) or Axio Cellobserver Z1 (Zeiss, Germany). Digital photomicrographs of DAB-staining and *in situ* hybridizations were taken using a light transmission microscope BX40 (Olympus, Germany) and a digital camera DP70 (Olympus, Germany). Photoshop CS5 was applied for editing images, while ImageJ software was used for cell number counting and measurements of the radial extension of cortical structures. Analysis was performed blindly. For quantification of the relative radial extension of cortical layers, coronal sections of the somatosensory cortex (Bregma: 0, interaural: 3.8 mm) were used. Immunohistochemistry against Cux2/Otx 1,2 in combination with DAPI nuclear labeling served to clearly distinguish between the infragranular layers 5/6 and the superficial layers 1, 2-4.

For quantification of cell staining in embryonic brains, coronal sections of the dorso-lateral cortex from sections with evident ganglionic eminences in the basal telencephalon were analyzed. For Tbr1, the thickness of the cortical plate (CP) was measured in comparison to the radial extension of the cortex. Moreover, we counted the number of Tbr1 positive cells normalized to a defined area. The division angle of apical progenitors at E13.5 was determined using Aspm-staining labeling cell poles in combination with DAPI nuclear staining illustrating the division plane. The angles between the division plane and the lateral ventricle were determined and classified into three groups. Angles within 60-90° were defined as vertical, 30-60° as oblique and 0-30°C as horizontal divisions. For Ki67, cell numbers in the transient, proliferative layers (VZ and SVZ) were counted and the proportional distribution was calculated.

For quantification of cortical progenitors at E16.5 and E18.5, a radial section of the dorso-lateral cortex was taken, divided horizontally in 20 equal segments and cells per segments were analyzed. For the analysis at E13.5, we divided the cortical section into 10 segments.

For analyzing the *Insm1*-signal, coronal sections of the dorso-lateral cortex were taken, and grey values were measured with ImageJ. Thereby, the darkest position was defined as 100% and the brightest position as 0%. The grey values were calculated relatively in percentage.

For the analysis of cell pairs formed in co-cultures with thalamic explants, only pairs located clearly within the axons were taken into consideration. The number of cell tracker green-positive pairs was counted, which consisted either of two nestin or two βIII-tubulin labeled cells or mixed pairs. The proportional incidents are illustrated in percentages.

For analyzing the number of Tbr2 positive cells in cortices of organotypic slices treated with ephrin A5-Fc- or Fc-coated beads, cells per section within the width of the beads were counted and normalized with flanking lateral and medial regions. The mean for all samples for Fc-protein- and ephrin A5-Fc-coated beads was calculated and the change in percentage is illustrated. The number "n" refers to the number of analyzed cells (single cell RT-PCR), cell pairs (pair cell assay and co-culture of thalamic explants with cortical single cells), explants or sections of at least three independent experiments. *Student´s t-test*, *Chi-Square test, One-way* and *Two-way ANOVA* as well as *Bonferroni test* were used for statistical analysis (*, $p<0.05$; **, $p<0.01$; ***, $p<0.001$.

Supplementary Figure Legends

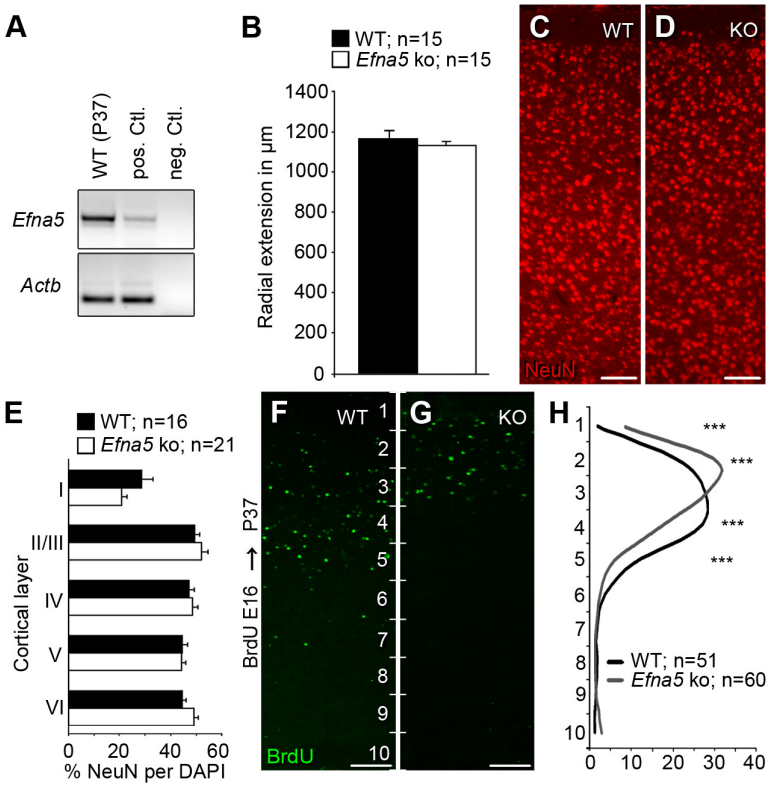

Supplementary Figure 1: Additional analysis of the adult *Efna5* and wildtype cortex.

A, Ephrin A5 (*EfnA5*) and β-actin (*ActB*) PCR of wildtype cortical tissue at P37. **B**, Quantitative analysis of the radial extension (from layer 6 to the pia) of the adult cortex at P37 reveals no differences between wildtype and *Efna5* knockout mice. **C-E**, Analysis of the neuronal density in wildtype (**C**) and *Efna5* mutant cortices (**D**) with NeuN (Rbfox3) immunohistochemistry. The percentage of NeuN (Rbfox3)-stained neurons per total cell number labeled with DAPI (not shown) was determined for the different cortical layers at P37 resulting in no significant differences neither by two-way *ANOVA* (n.s., p=0.93) nor by *Bonferroni Test* for the different layers (3 brains per genotype) (**E**). **F-H**, BrdU birthdating experiments were performed to follow the fate of late born neurons at E16.5. The distribution of BrdU-labeled layer 2-4 cells in the adult wildtype (**F**) and *Efna5* knockout (**G**) somatosensory cortex at P37 revealed a shift towards the pia and a reduction in the radial extension of BrdU labeled cells in the knockouts (**H**; *Bonferronie Test*; ***, p<0.001 for segment 1, 2, 4, 5). Scale bars: 100 µm in **C**, **D**, **F**, **G**.

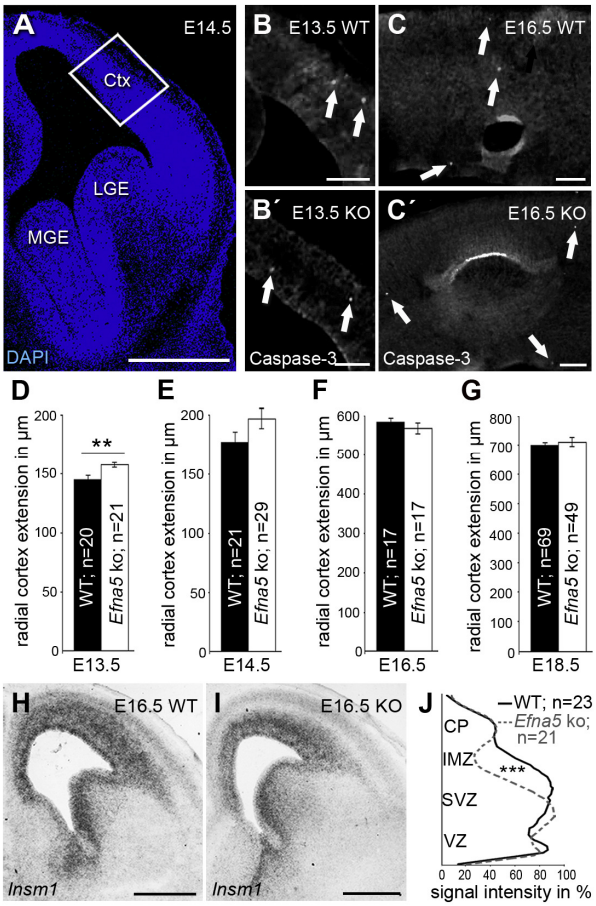

Supplementary Figure 2: Additional analysis of the embryonic *Efna5* and wildtype cortex

A, The white rectangle in the DAPI stained E14.5 coronal section illustrates the dorso-lateral part of the neocortex used for analysis at embryonic stages. **B-C´**, Immunostaining against Caspase-3 in coronal sections of E13.5 and E16.5 wildtype (**B**, **C**) and *Efna5* deficient embryos (**B´**, **C´**) revealed no apparent differences. **D-G**, The radial extension of the dorso-lateral cortex was measured in wildtype and *Efna5* deficient embryos at E13.5 (**D**; 2 brains per genotype), E14.5 (**E**; 3 brains per genotype), E16.5 (**F**; 2 brains per genotype) and E18.5 (**G**; 4 brains for wildtype and 2 brains for *Efna5* deficient embryos). At E13.5 the radial extension of *Efna5* deficient cortices was significantly increased (*Student´s t-test*; **, p≤0.01), while no differences were observed at E14.5-E18.5. **H-J**, *In situ* hybridization against *Insm1* in WT (**H**; 2 brains) and *Efna5* knockout (**I**; 3 brains) E16.5 coronal sections revealed significantly decreased signal intensities in the SVZ of mutant cortices (**J**; two-way *ANOVA*; ***, p≤0.001). In **D-G**, **J**, "n" refers to the number of analyzed sections. Ctx=cortex, *Insm1*=insulinoma associated 1, LGE=lateral ganglionic eminence, MGE=medial ganglionic eminence. Scale bar: 500 µm in **A**, **H, I**; 100 µm in **B -C´**.

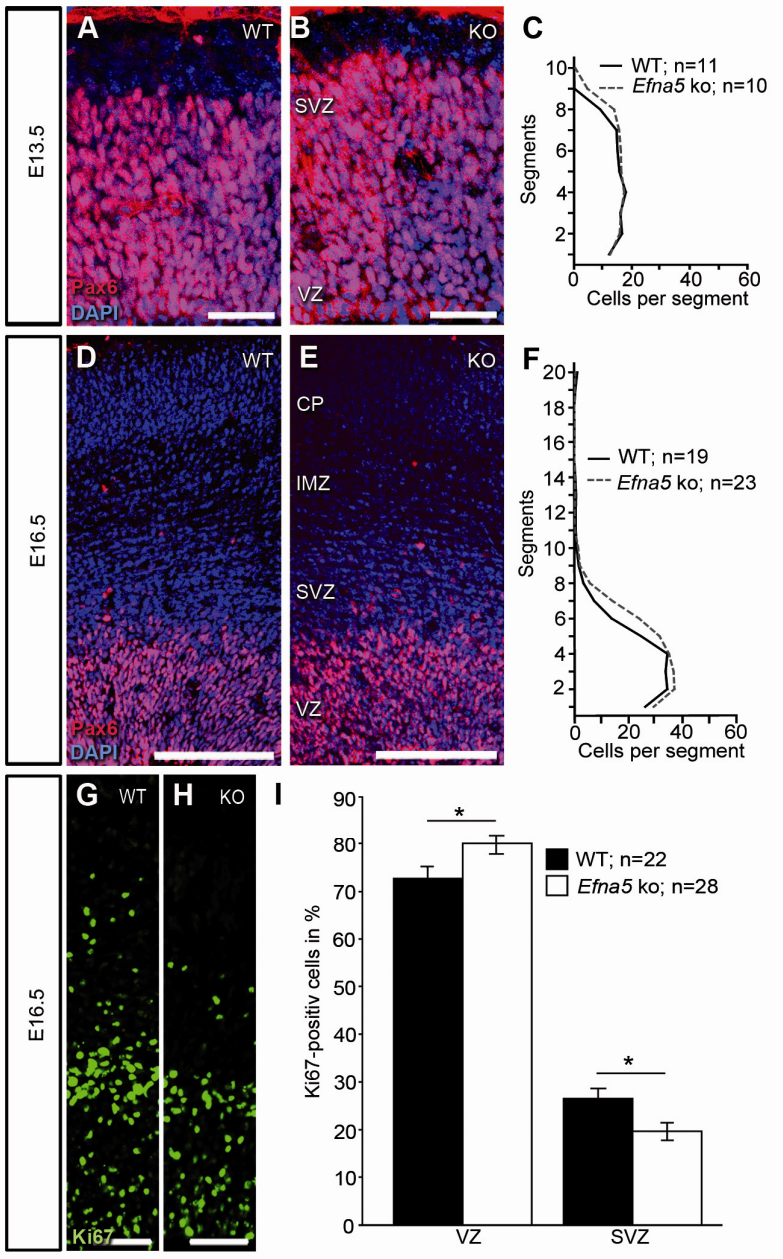

Supplementary Figure 3: Pax6 and Ki67 immunostaining in the embryonic *Efna5* and wildtype cortex.

A-F, Overlay of Pax6 immunostaining (red) and DAPI labeling (blue) in coronal sections of the E13.5 (**A**, **B**) and E16.5 (**D**, **E**) cortices. At E13.5, two-way *ANOVA* analysis revealed no differences between wildtype (**A**) and *Efna5* knockout embryos (**B**) as quantified in **C** (n.s., p=0.168; 2 brains per genotype). The cell number in segments 8 and 9 were increased as

revealed by *Bonferroni Test* (**, p≤0.01). At E16.5, two-way *ANOVA* analysis also revealed no significant changes in *Efna5* knockouts (**E**) compared to wildtypes (**D**), as quantified in **F** (n.s., p=0.093; 3 brains per genotype). Yet, by applying *Bonferronie Test* increased number in segments 5-7 (**, p<0.01 for segments 5 and 7; ***, p≤0.001 for segment 6) were observed in *Efna5* knockout brains. **G-I**, Immunostaining in sections of E16.5 cortices against Ki67 revealed a decreased proportion of basally dividing cells in the SVZ of *Efna5* deficient mice (**H**) compared to wildtypes (**G**) as quantified in **I** (*, p<0.05, *Student´s t-test,* 3 brains per genotype). Number "n" refers to the number of analyzed sections. VZ=ventricular zone, SVZ=subventricular zone, IMZ=intermediate zone, CP=cortical plate. Scale bars: 100 µm in **D**, **E**, 50 µm in **A**, **B**, **G** and **H**.

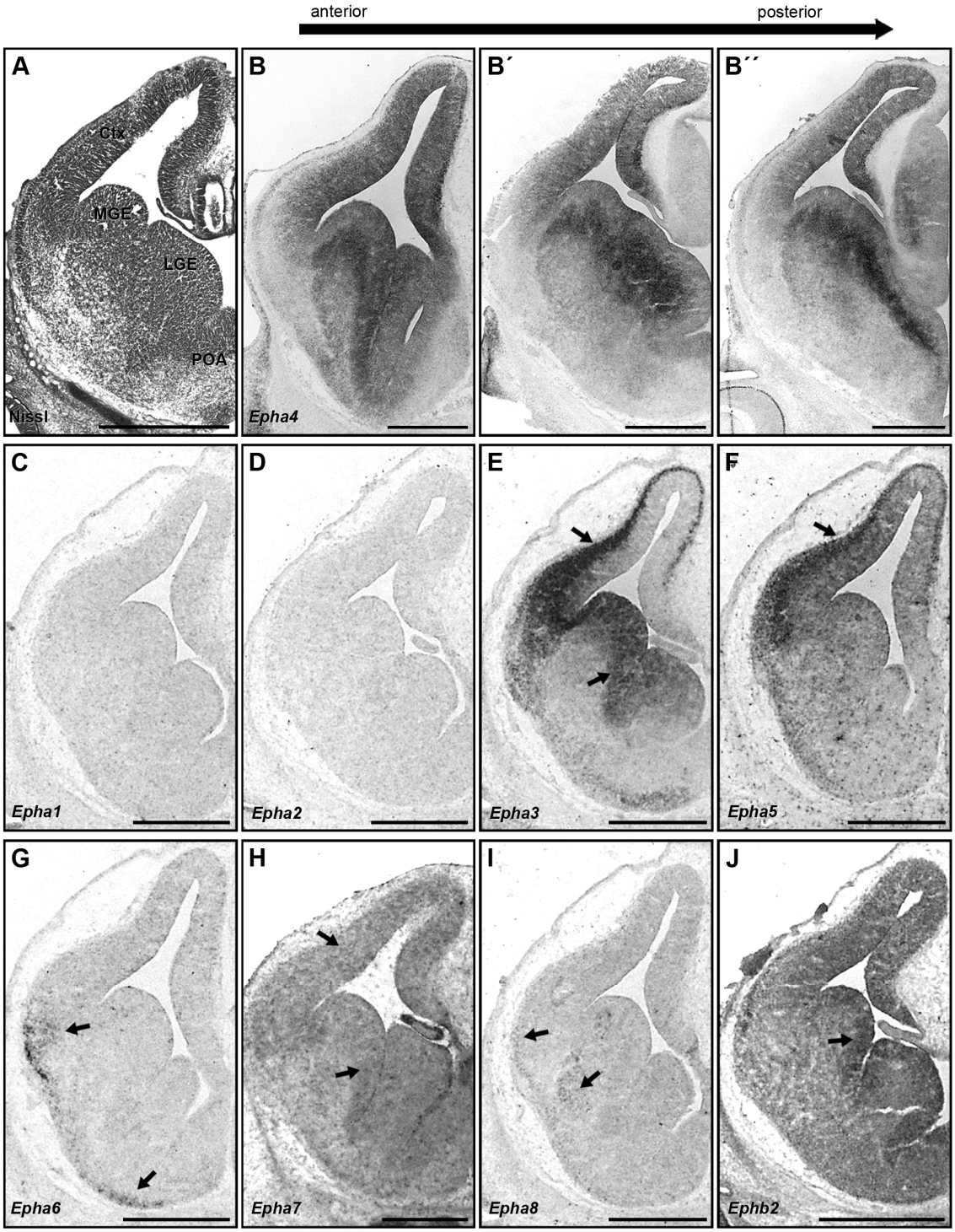

Supplementary Figure 4: Eph-receptor expression analysis in the E14.5 wildtype cortex

A, Nissl stained E14.5 coronal section of the embryonic brain. **B-B´´**, *Epha4* is expressed in the proliferative zones of the developing cortex (E14.5) in anterior, medial as well as

posterior sections. The ephrin A5-affine receptors *Epha1* (**C**), *Epha2* (**D**), *Epha6* (**G**), *Epha7* (**H**), *Epha8* (**I**), and *Ephb2* (**J**) are not expressed in the developing neocortex (E14.5). *Epha3* (**E**) and *Epha5* (**F**) are expressed in the cortical plate, but not in the transient proliferative zones of the dorsal telencephalon (E14.5). Ctx=cortex, LGE=lateral ganglionic eminence, MGE=medial ganglionic eminence, POA=preoptic area. Scale bars: 500 µm in **A-J**.

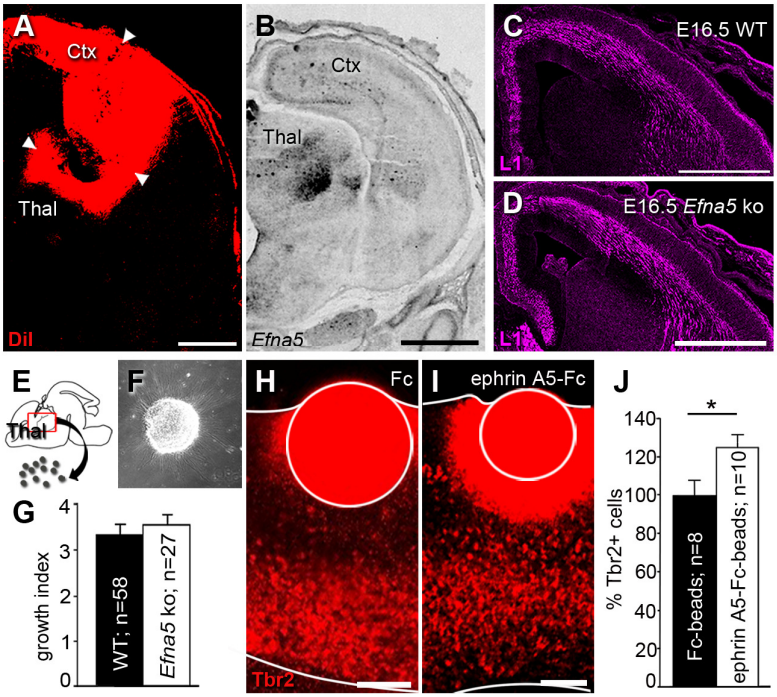

Supplementary Figure 5: Thalamic ephrin A5 influences the generation of IPCs.

A, **B**, DiI crystal placed in the dorso-lateral embryonic cortex at E16.5 (**A**) retrogradely tags the thalamic region which expresses *Efna5* as shown with *in situ* hybridization (**B**). **C**, **D**, L1-immunostaining was performed in coronal sections of E16.5 wildtype (**C**) and *Efna5* mutant brains (**D**) to label thalamo-cortical projections in the developing cortex, which did not reveal alterations in *Efna5* deficient brains. **E-G**, thalamic explants (E14.5+1div) prepared from wildtype and *Efna5* knockout embryos did not show significant differences in the axonal outgrowth index (2 independent experiments for wildtype and knockout tissue). **H-J**, Tbr2 immunostaining of organotypic slices of *Efna5*-deficient brains (E14.5 + 2 days *in vitro*). Fc-protein-coated (**H**) or ephrin A5-Fc-coated protein-A-agarose beads (**I**) were placed in the CP/IMZ of the cortex, revealing an increase in Tbr2-positive cells in response to exogenous ephrin A5 (**J**; *Student´s t-test*; *, $p<0.05$; 3 independent experiments). For quantification, Tbr2-positive cells in slices treated with Fc-protein-coated beads were set to 100%. Number "n" refers to the number of analyzed explants in **G** and analyzed sections in **J**. Ctx=cortex, Thal=thalamus, CP=cortical plate, IMZ=intermediate zone. Scale bars: 500 µm in **A-D**; 50 µm in **H**, **I**.

Supplementary References

Iscove, N. N., Barbara, M., Gu, M., Gibson, M., Modi, C. and Winegarden, N. (2002). Representation is faithfully preserved in global cDNA amplified exponentially from sub-picogram quantities of mRNA. *Nature biotechnology* **20**, 940-943.

Zimmer, G., Kastner, B., Weth, F. and Bolz, J. (2007). Multiple effects of ephrin-A5 on cortical neurons are mediated by SRC family kinases. *The Journal of neuroscience : the official journal of the Society for Neuroscience* **27**, 5643-5653.